

Self-interaction and relaxation-corrected pseudopotentials for II-VI semiconductors

Dirk Vogel, Peter Krüger, and Johannes Pollmann

Institut für Theoretische Physik II, Universität Münster, D-48149 Münster, Germany

(Received 22 February 1996)

We report the construction of pseudopotentials that incorporate self-interaction corrections and electronic relaxation in an approximate but very efficient, physically well-founded, and mathematically well-defined way. These potentials are particularly useful for II-VI compounds which are distinguished by their highly localized and strongly bound cationic semicore d electrons. Self-interaction corrections to the local-density approximation (LDA) of density-functional theory are accounted for in the solids to a significant degree by constructing appropriate self-interaction-corrected (SIC) pseudopotentials that take *atomic* SIC contributions into account. In this way translational symmetry of the Hamiltonian is preserved. Without increasing the complexity of the numerical calculations we approximately account, in addition, for electronic relaxation in the solids by incorporating into our pseudopotentials relevant relaxation in the involved *atoms*. By this construction we arrive at very useful self-interaction and relaxation-corrected pseudopotentials and effective one-particle Hamiltonians which constitute the basis for *ab initio* LDA calculations yielding significant improvements in electronic properties of II-VI compound semiconductors and their surfaces. The procedure is computationally not more involved than any standard LDA calculation and, nevertheless, overcomes to a large extent the well-known shortcomings of “state of the art” LDA calculations employing standard pseudopotentials. Our results for electronic and structural properties of II-VI compounds agree with a whole body of experimental data. [S0163-1829(96)02832-9]

I. INTRODUCTION

Most current electronic structure calculations treat systems of many interacting electrons within the density-functional theory (DFT) of Hohenberg, Kohn, and Sham^{1,2} by employing the local-density approximation (LDA) or the local spin density (LSD) approximation, respectively. Due to its formal and computational simplicity, as well as its very impressive successes in describing ground-state properties of many-electron systems, DFT-LDA has become the dominant approach for calculating structural and electronic properties of bulk semiconductors and their surfaces. For semiconductors the approach is now most often applied in conjunction with “state of the art” nonlocal, norm-conserving pseudopotentials. Although the eigenvalues of the Kohn-Sham equations as formal Lagrangian multipliers do not have a direct physical meaning, except for the highest occupied eigenvalue,^{3,4} their interpretation as electronic excitation energies has led to remarkable results in band-structure theory of solids. Nevertheless, calculated electronic properties resulting from such LDA calculations show a number of systematic shortcomings. The most apparent deficiency in many semiconductors and insulators is the underestimate of band gaps by typically 50% or more. This shortcoming is even more severe in II-VI compound semiconductors. We find, e.g., a LDA band gap E_g^{th} of only 0.23 eV for ZnO (Ref. 5) as opposed to the experimental value of $E_g^{\text{expt}}=3.44$ eV. This unusually large underestimate of the gap energy is intimately related to another very severe shortcoming of standard LDA calculations. They also fail to accurately describe strongly localized semicore d states and underestimate their binding energies. This is partially due to unphysical self-interactions and to the neglect of electronic relaxation contained in any standard LDA calculation. Especially in the case of II-VI

semiconductors, the d -electron bands have been found in many LDA calculations⁵⁻¹² to occur some 3 eV too high in energy as compared to experiment.¹³⁻¹⁷ In consequence, their interactions with the anion p valence bands are artificially enlarged, falsifying the dispersions and bandwidth of the latter and shifting them inappropriately close to the conduction bands. As a result, the LDA band-gap underestimate is even significantly more pronounced for II-VI compounds than for elemental or III-V semiconductors.

Since electronic and structural properties of II-VI compound semiconductors, their surfaces and interfaces, are currently moving into the focus of interest because of their paramount technological potential in optoelectronics and catalysis, one would like to have a more accurate theoretical approach for their treatment available. A reliable description of valence- and conduction-band states, in particular, near the gap energy region, is mandatory for meaningful calculations of defect properties in II-VI bulk semiconductors, band-edge properties in ternary or quaternary II-VI compounds, and electronic properties of II-VI compound semiconductor surfaces and interfaces. Strongly misplaced d bands significantly influence the anion p valence bands and the gap energy. Therefore very accurate calculations for the systems mentioned above by a straightforward application of standard pseudopotential LDA cannot be achieved. Of course, one could study such systems using quasiparticle band-structure calculations¹⁸⁻²² including semicore d electrons explicitly within the GW approximation. Such calculations have very recently been shown to be feasible, indeed, for cubic bulk CdS (Ref. 21) and ZnSe (Ref. 22) but they are very involved already for bulk crystals and forbiddingly involved for II-VI semiconductor surfaces or interfaces.

From the work of Perdew and Zunger²³ on free atoms and ions it is well known that self-interactions, being most pro-

nounced for tightly bound and highly localized states, give rise to significant misplacements of respective energy levels. Self-interaction corrections (SIC) including orbital relaxation can easily be incorporated²³ in electronic structure calculations for atoms within LDA or its spin-polarized variant, the LSD approximation. But even SIC-LSD calculations fail to yield exact binding energies of all atomic states because they do not fully take into account *electronic* relaxation. Very accurate atomic binding energies can be obtained, however, within the so-called delta self-consistent field (Δ SCF) approach.²⁴ Δ SCF binding energies are derived from well-defined total-energy *difference* calculations for ground states of neutral and ionized atoms, avoiding to a great extent problems originating from the neglect of electronic relaxation as contained in standard LDA calculations. But for solids such Δ SCF calculations are not practicable to date.

If the SIC formalism is extended to solids, it gives rise to orbital-dependent effective potentials which no longer have the translational invariance of the original Bravais lattice. Extended Bloch orbitals lead to nearly homogeneous one-particle densities and to vanishing SIC contributions. Appropriately localized wave functions, on the contrary, can yield strong SIC contributions within full SIC-LSD calculations. To avoid the practical problems involved in SIC-LSD calculations for solids, the method has been applied previously in simplified forms (see, e.g., Ref. 25, and the references therein). More recently, self-consistent SIC-LSD calculations have been reported, e.g., for bulk transition metals, high- T_c superconductors, Ce compounds, and transition-metal oxides by Svane and Gunnarson,^{26–28} Szotek, Temmermann, and Winter,^{29–31} and Arai and Fujiwara,¹¹ respectively. The work of these authors has clearly shown that SIC shifts occupied d states significantly down in energy also in solids. In consequence, it would be highly desirable to carry out full SIC-LDA calculations for II-VI semiconductors. We have investigated the feasibility of such calculations for wurtzite crystals which have four atoms per bulk unit cell. It turned out that such calculations would be extremely involved for the bulk already and they are currently entirely out of reach for surfaces or interfaces of zinc-blende (ZB) or wurtzite (W) II-VI semiconductors.

From a more general point of view the question then arises whether unphysical self-interactions can be corrected for and electronic relaxation can be taken into account within an alternative approach that is less involved. This is possible, indeed, as we will show. We have devised an efficient theoretical framework that accounts in an approximate way for both effects but, nevertheless, accurately describes electronic and structural properties of II-VI semiconductor compounds. A preliminary account of results obtained employing this approach has been published recently.³²

The basic idea on which we have built our approach is to construct *pseudopotentials* that take *atomic* self-interaction corrections and electronic relaxation in the constituent *atoms* into account from the very beginning. The idea to construct SIC-pseudopotentials (PPs) is not new, in principle. It was employed a long time ago in approximate SIC-LSD calculations for atoms and ions by Zunger³³ and more recently, e.g., for bulk Ge by Rieger and Vogl.³⁴ But the actual ways to construct SIC-PPs in the previous publications are largely different from our approach. We correct for the self-

interactions in the atoms in exactly the same way as described by Perdew and Zunger in their original SIC publication.²³ In addition, we take electronic relaxation in the atoms into consideration by referring to atomic Δ SCF results. Once our pseudopotentials are generated, they can be transferred to solids in an appropriate and well-defined way and can be employed in a standard LDA code. Our approach is capable of overcoming the above-mentioned LDA problems and is, nevertheless, computationally not more involved than any current “state of the art” LDA calculation. The electronic and structural properties calculated with our pseudopotentials are in gratifying agreement with a host of experimental data on II-VI compounds.

In Zunger’s early SIC-PP approach for atoms and ions³³ SIC corrections for the valence electrons were *not* incorporated in the SIC pseudopotential but they were explicitly taken into account. For atoms and ions this can be done without any practical problems. But the extension of that approach to solids is not straightforward and has, to the best of our knowledge, not been reported to date. Rieger and Vogl³⁴ have generated SIC pseudopotentials by fully taking into account the SIC-induced change of the Ge $3d$ core-charge density in the construction. The effect of the related corrections on the pseudopotential is noticeable. It leads to improved gap energies at the L , Γ , and X points of the Brillouin zone of Ge. The SIC-induced shifts of the lowest conduction band were found to be nonrigid and \mathbf{k} dependent. Our construction of pseudopotentials is distinctly different from those approaches, as will be shown in detail below.

In a recent publication, Zhang, Wei, and Zunger¹² have presented a broken-symmetry approach to the core hole in II-VI semiconductors in order to better describe d -band excitations in these solids. Their work is based on Slater’s “transition-state” concept³⁵ and refers to Δ SCF calculations in large supercells. For Zn-based IIB-VI semiconductors the authors obtain d -band energies which agree with the experimental values within 0.5–0.8 eV. Convergence of the results with respect to supercell size is relatively slow, however, so that the calculations are fairly involved for bulk compounds already. It may be complicated, therefore, to actually apply that approach to surfaces or interfaces. Such applications are straightforward, on the contrary, in our approach.

Our paper is organized as follows. In Sec. II we describe the construction of our pseudopotentials. Section III is devoted to the presentation and discussion of the results of our applications of these pseudopotentials to II-VI semiconductors. In Sec. IV we describe the calculation of the total energy, of lattice constants, and bulk moduli within our approach and present results for a number of compounds. A brief summary together with a short outlook concludes the paper in Sec. V. Some important formal details are given in the Appendix.

II. THEORETICAL APPROACH

In this section we first show the motivation of our approximate approach for taking self-interaction corrections and electronic relaxation into account. In this context we address basic properties of the constituent atoms of the studied compounds. Then we describe how the pseudopotentials are actually constructed.

TABLE I. Experimental ionization energies E_{expt} (from Ref. 40) and atomic term values $\tilde{\epsilon}$ as resulting from all-electron LSD and SIC-LSD, as well as all-electron LDA and SIC-LDA calculations. The term values $\tilde{\epsilon}_{\text{LDA}}^{\text{SIC-PP}}$ resulting from standard LDA calculations according to Eq. (5) employing our SIC-PPs are given for further reference, as well. Binding energies E as resulting from our LSD- and LDA- Δ SCF calculations are also given.

	E_{expt}	$\tilde{\epsilon}_{\text{all-el}}^{\text{LSD}}$	$\tilde{\epsilon}_{\text{all-el}}^{\text{SIC-LSD}}$	$E_{\text{all-el}}^{\text{LSD-}\Delta\text{SCF}}$	$\tilde{\epsilon}_{\text{all-el}}^{\text{LDA}}$	$\tilde{\epsilon}_{\text{all-el}}^{\text{SIC-LDA}}$	$E_{\text{all-el}}^{\text{LDA-}\Delta\text{SCF}}$	$\tilde{\epsilon}_{\text{LDA}}^{\text{SIC-PP}}$
Zn 4s	-9.4	-6.2	-9.3	-9.9	-6.2	-9.3	-9.9	-9.4
3d	-17.2	-10.4	-20.0	-17.9	-10.4	-20.0	-17.9	-20.0
Cd 5s	-9.0	-6.0	-8.9	-9.4	-6.0	-8.9	-9.4	-8.9
4d	-17.6	-11.9	-18.9	-18.0	-11.9	-18.9	-18.0	-18.7
O 2p	-13.6	-7.5	-14.5	-14.0	-9.2	-16.5	-16.2	-16.5
2s	-28.5	-21.9	-29.1	-28.8	-23.8	-31.0	-30.9	-31.2
S 3p	-10.4	-6.3	-10.5	-10.6	-7.1	-11.4	-11.6	-11.4
3s	-20.3	-16.3	-21.4	-21.2	-17.3	-22.4	-22.4	-22.5
Se 4p	-9.8	-6.0	-9.7	-10.0	-6.7	-10.5	-10.8	-10.5
4s	-20.2	-16.7	-21.5	-21.5	-17.5	-22.3	-22.4	-22.4
Te 5p	-9.0	-5.6	-8.8	-9.1	-6.1	-9.4	-9.8	-9.4
5s	-17.8	-14.8	-18.9	-19.0	-15.4	-19.5	-19.7	-19.5

A. Motivation of the approach

The LSD approximation of density-functional theory simplifies the approximate calculation of ground-state properties of a many-electron system with charge density $n(\mathbf{r})=n_{\uparrow}(\mathbf{r})+n_{\downarrow}(\mathbf{r})$ by mapping the many-particle Schrödinger equation onto effective one-particle equations,^{1,2}

$$H_{\text{eff},\sigma}^{\text{LSD}}\psi_{\alpha\sigma}=\tilde{\epsilon}_{\alpha\sigma}^{\text{LSD}}\psi_{\alpha\sigma},$$

$$H_{\text{eff},\sigma}^{\text{LSD}}[n]=-\nabla^2+V_{\text{ext}}+V_{\text{Coul}}[n]+V_{\text{xc},\sigma}^{\text{LSD}}[n_{\uparrow},n_{\downarrow}], \quad (1)$$

$$E^{\text{LSD}}[n_{\uparrow},n_{\downarrow}]=\sum_{\alpha,\sigma}^{\text{occ}}\tilde{\epsilon}_{\alpha\sigma}^{\text{LSD}}-\frac{1}{2}\int V_{\text{Coul}}[n]n(\mathbf{r})d^3r$$

$$+E_{\text{xc}}^{\text{LSD}}[n_{\uparrow},n_{\downarrow}]$$

$$-\sum_{\sigma}\int V_{\text{xc},\sigma}^{\text{LSD}}[n_{\uparrow},n_{\downarrow}]n_{\sigma}(\mathbf{r})d^3r,$$

which can be solved iteratively.³⁶ Within LSD, the inadequate description of localized states arises to a large extent from unphysical self-interactions inherent in the approximation, as has been shown by Perdew and Zunger.²³ These authors have suggested accounting for unphysical self-interactions by adding a correction term to the LSD energy functional, which then reads

$$E^{\text{SIC-LSD}}[n_{\uparrow},n_{\downarrow}]=E^{\text{LSD}}[n_{\uparrow},n_{\downarrow}]$$

$$-\sum_{\alpha,\sigma}^{\text{occ}}\left[\frac{1}{2}\int V_{\text{Coul}}[n_{\alpha\sigma}]n_{\alpha\sigma}(\mathbf{r})d^3r\right.$$

$$\left.+E_{\text{xc}}^{\text{LSD}}[n_{\alpha\sigma},0]\right]. \quad (2)$$

The correction term gives a remarkable contribution to the total energy if the one-particle densities $n_{\alpha\sigma}$ are strongly localized but vanishes if they are completely homogeneous. According to the variational principle, the SIC-LSD energy functional (2) can be minimized by an iterative solution of the related all-electron SIC-LSD equations

$$(H_{\text{eff},\sigma}^{\text{LSD}}-V_{\text{Coul}}[n_{\alpha\sigma}]-V_{\text{xc}}^{\text{LSD}}[n_{\alpha\sigma},0])\psi_{\alpha\sigma}$$

$$=\sum_{\alpha'}^{\text{occ}}\lambda_{\alpha,\alpha'}^{\sigma}\psi_{\alpha'\sigma}. \quad (3)$$

For the total energy of atoms it has been shown that SIC-LSD results are in much better agreement with experimental data than LSD results.^{23,37,38} In addition, atomic eigenvalues resulting from Eq. (3) are in much better agreement with measured binding energies than LSD eigenvalues, which typically underestimate the measured energies by some 40% (see, e.g., Refs. 23, 25, and 39, and the references therein). In spite of the very encouraging SIC-LSD results for atoms the approach has not widely been used in solid-state calculations, so far, because applications of the SIC-LSD formalism to solids are extremely demanding, as we have pointed out in the Introduction.

In our alternative approach the very involved self-consistent determination of appropriately localized one-particle orbitals and resulting SIC potentials *for the solid* is avoided. Our SIC potentials need to be calculated only once for the atoms and are consecutively transferred to the solids. To construct our pseudopotentials we need to have the most accurate atomic energies available as a reliable reference. Therefore we have first calculated all-electron LSD and SIC-LSD eigenvalues and eigenfunctions for all constituent atoms of the II-VI compounds considered in this work. The resulting eigenvalues are given in Table I. In our solid-state calculations, to be described further below, we can employ the LDA instead of the LSD approximation because we are only concerned with systems that exhibit no spin polarization. Therefore we have calculated for further reference the respective all-electron LDA and SIC-LDA eigenvalues and eigenfunctions for the related atoms, as well. The respective eigenvalues are also included in Table I. For further comparison the table shows, in addition, measured ionization energies⁴⁰ and calculated Δ SCF binding energies which we have obtained from all-electron LSD or LDA calculations, respectively. We have also calculated respective Δ SCF energies within SIC-LDA and SIC-LSD. They are in slightly less

favorable agreement with experiment and therefore are not considered further in this work as a reference.

There are a number of points to be stressed in connection with the results in Table I which are most relevant for our construction of appropriate pseudopotentials. First, we note that the all-electron LSD results are largely at variance with the experimental data. The all-electron SIC-LSD results considerably improve on the comparison. The highest occupied orbital energies (except for O $2p$) are in very good agreement with the experimental ionization energies, indeed, as has already been discussed in detail by Perdew and Zunger.²³ But there still occur significant differences, most noticeably concerning the semicore d states of Zn and Cd, as well as the s core states of S, Se, and Te. The calculated all-electron LSD- Δ SCF binding energies of the d states agree considerably better with experiment. We note in this context that LSD- Δ SCF leads to some extent to an overbinding of all states, as is obvious in Table I. But the differences between Δ SCF binding energies of different states of particular atoms, which are solely relevant in a solid-state calculation, are almost in exact agreement with experiment for Zn, Cd, and O and they only deviate by roughly 1 eV from experiment for S, Se, and Te. Comparing respective all-electron SIC-LSD eigenvalues with the LSD- Δ SCF binding energies, we observe that the differences are of the order of 0.6 eV or less for most of the states while they amount to 2.1 eV for the Zn $3d$ and 0.9 eV for the Cd $5d$ states. Even more interestingly, the differences between the Zn $4s$ -Zn $3d$ and Cd $5s$ -Cd $4d$ energies as resulting from LSD- Δ SCF agree with experiment within 0.2 eV while the respective SIC-LSD eigenvalue differences deviate by 2.9 eV for Zn and 1.4 eV for Cd from experiment. These deviations of the SIC-LSD results from experiment are expected to largely be due to the neglect of electronic relaxation in that approach. The relaxation is fully taken into account in LSD- Δ SCF only. It is most pronounced for highly localized states (e.g., Zn $3d$). All above general comments on the LSD results apply equally well to our respective LDA results. For the Zn and Cd atoms these are identical, anyway, because there is no spin polarization in the closed shells of the $[\text{Ar}]3d^{10}4s^2$ and $[\text{Kr}]4d^{10}5s^2$ configurations. In the open valence shells of O, S, Se, and Te with their [rare gas] np^4ns^2 configurations with $n=2, 3, 4,$ and $5,$ respectively, strong spin-polarization effects are to be observed. The respective binding energies, as resulting from the LSD- Δ SCF and LDA- Δ SCF calculations, differ by about 2.2, 1.1, 0.8, and 0.7 eV, respectively.

Our approach to describing SIC contributions in *II-VI compounds* approximately by taking only respective atomic SIC contributions into account may seem fairly crude, at a first glance. But there are strong indications for the meaningfulness of such an approach. First, the underbinding of d bands in standard LDA results is roughly of the same size for different compounds irrespective of their different lattice constants.⁵⁻¹² This is considered as a strong hint to the fact that atomic effects are mainly responsible for the deviations. Second, the bulk pseudocharge densities of all our investigated *II-VI* compounds only slightly differ from respective superpositions of atomic pseudocharge densities. As an example we show a direct comparison of respective pseudocharge densities of ZnO in Fig. 1. The agreement is very close, and it is even closer for CdS (see Ref. 41). Therefore

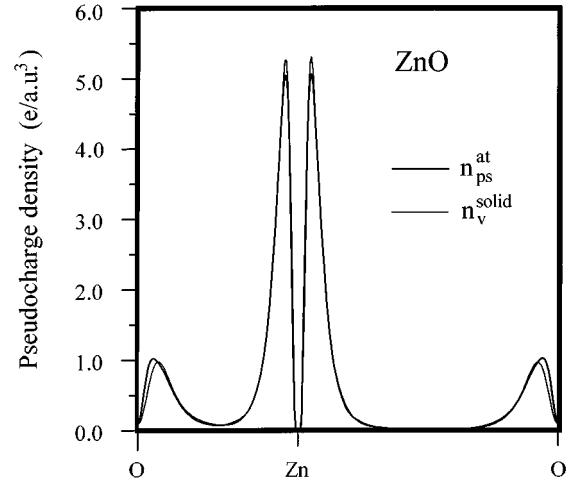


FIG. 1. Comparison of the pseudocharge density along the Zn-O bond direction in bulk ZnO with the respective superposition of atomic Zn and O pseudocharge densities.

it is possible to separate the bulk valence charge density into localized one-particle orbital densities which are nearly identical to the respective atomic one-particle orbital densities and thus should lead to similar SIC contributions in the solid as in the related atoms. In addition, the band structure of *II-VI* compound semiconductors is dominated by atomic effects. It is built up of separated band groups with nearly atomic character.⁵⁻¹² The transfer of atomic SIC potentials to the solid is therefore expected to give rise to shifts of the single band groups similar to the SIC-induced shifts of the respective atomic energy levels (see Table I). To highlight the expected SIC effects on the bulk band structures we have schematically drawn in Fig. 2 the various band groups as resulting from LDA calculations and we have indicated the *expected* shifts of the band groups according to SIC-LDA. Note that the SIC-induced *downward* shift of all occupied band groups has appropriately been accounted for in the schematic drawing. These shifts should remedy the deficiencies of LDA calculations using standard pseudopotentials to a considerable extent. An appropriate transfer of atomic SIC contributions to the solid by appropriately constructed pseudopotentials therefore seems very promising.

B. Construction of pseudopotentials

We first solve the one-particle all-electron SIC-LDA equations for the involved *atoms*,

$$\left(-\nabla^2 - \frac{2Z}{r} + V_{\text{Coul}}[n] + V_{\text{xc}}^{\text{LDA}}[n] - V_{\text{Coul}}[n_{\alpha}] - V_{\text{xc}}^{\text{LSD}}[n_{\alpha}, 0] \right) \psi_{\alpha} = \tilde{\epsilon}_{\alpha}^{\text{SIC}} \psi_{\alpha}. \quad (4)$$

The exchange-correlation potential in the SIC term enters in the spin-polarized form since SIC depends on the charge densities of the particular states involved. In our calculations for the atoms we apply the original SIC-LDA or SIC-LSD formalism, respectively, as proposed by Perdew and Zunger.²³ Using this formalism, the orbitals can result as

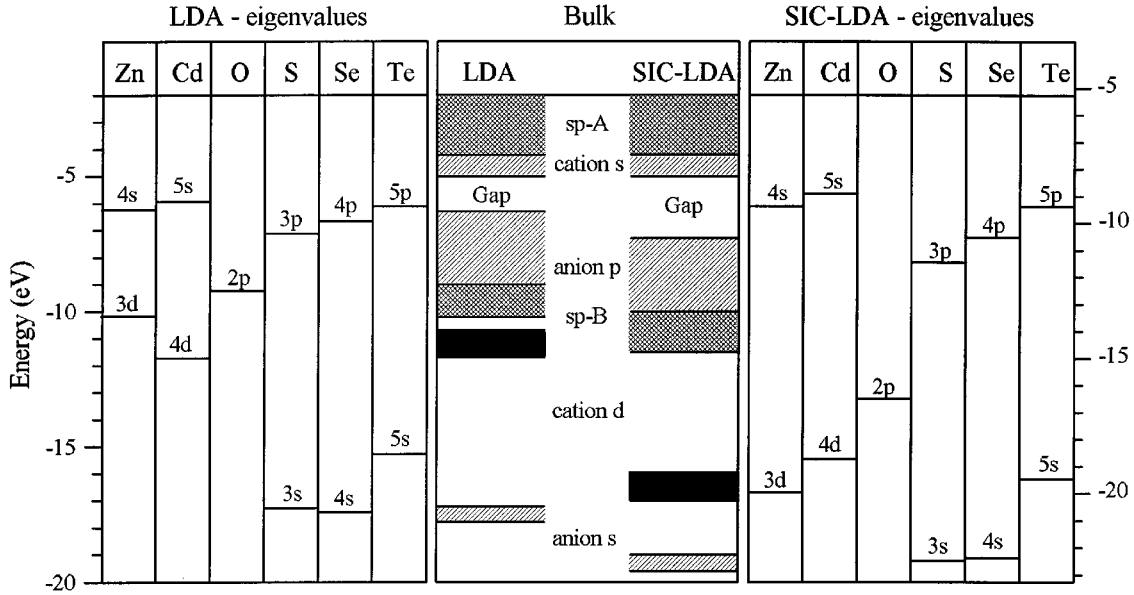


FIG. 2. Comparison of the *atomic* term values from Table I as resulting from all-electron LDA (left panel) and all-electron SIC-LDA calculations (right panel). Note the difference in energy scales for the two panels. Apart from a rigid shift of all SIC-LDA term values to lower energies relative to the LDA term values, distinctive changes in the *term-value differences* resulting from the two calculations are to be noted. The latter are of paramount importance for the solid-state calculations. The bands that can be expected to result from corresponding solid-state calculations are schematically indicated on the left- and right-hand side of the middle panel, respectively. In addition to cation *s* and *d* bands, as well as anion *s* and *p* bands, there are also *sp*-antibonding (*sp-A*) and -bonding (*sp-B*) bands.

slightly nonorthogonal but for *atoms* the influence of the nondiagonal elements of $\lambda_{\alpha,\alpha'}^\sigma$ and the resulting nonorthogonality effects are very small.

1. SIC pseudopotentials

Next, we replace the all-electron Coulomb potential $-2Z/r$ in Eq. (4) by an ionic pseudopotential $V_{ps,\alpha}$ and solve the resulting equations for the respective *pseudoatoms*,

$$\begin{aligned} & (-\nabla^2 + V_{ps,\alpha} - V_{Coul}[n_\alpha^{at}] - V_{xc}^{LSD}[n_\alpha^{at}, 0]) \\ & + V_{Coul}[n_v] + V_{xc}^{LDA}[n_v]) \Phi_\alpha^{ps} = \tilde{\epsilon}_{ps,\alpha}^{SIC} \Phi_\alpha^{ps}, \end{aligned} \quad (5)$$

where n_v is the total pseudocharge density of the valence electrons,

$$n_v(\mathbf{r}) = \sum_{\alpha}^{occ} |\Phi_\alpha^{ps}(\mathbf{r})|^2, \quad (6)$$

and n_α^{at} is the atomic pseudocharge density of orbital α . We now define the first three potential terms in Eq. (5) as our SIC pseudopotentials, which are thus given as

$$\tilde{V}_{ps,\alpha}^{SIC} := V_{ps,\alpha} - V_{Coul}[n_\alpha^{at}] - V_{xc}^{LSD}[n_\alpha^{at}, 0] =: V_{ps,\alpha} + \delta\tilde{V}_\alpha^{SIC}. \quad (7)$$

This definition of SIC-PPs is different from that in the early approach of Zunger.³³ For the reasons discussed above we employ atomic orbital charge densities in the SIC terms of Eq. (7) while Zunger used orbital-charge densities calculated for the new chemical environment. The latter are readily available in the small systems which he studied. The first term, $V_{ps,\alpha}$, describes the influence of the nucleus and the core on the valence electrons. For this part of our pseudo-

potentials we employ ionic nonlocal norm-conserving pseudo-potentials $V_{ps,\alpha}^{LDA}$ from the literature^{42,43} which are used in our standard LDA calculations as well. We thus neglect the SIC influence on the charge density of low-lying core electrons. This is quite complementary to the approach of Rieger and Vogl.³⁴ For the energetically low-lying core states in II-VI compounds it turns out to be well justified, however, as we will point out further below. The second part, $\delta\tilde{V}_\alpha^{SIC}$, is the SIC contribution of valence electron α as defined in Eq. (4). In contrast to the common pseudopotential concept, our SIC pseudopotentials contain not only information about the nucleus and the core electrons but also have distinct information about the behavior of the valence electrons in the *pseudoatoms*.

Solving Eq. (5) for the pseudoatoms with $V_{ps,\alpha} = V_{ps,\alpha}^{LDA}$, it turns out that the resulting pseudo-eigenvalues agree already remarkably well, mostly within 0.1 eV, with the all-electron SIC-LDA eigenvalues resulting from Eq. (4), as can be seen in Table I. In addition, the eigenfunctions fulfill to a very high degree all conditions that are usually required for the pseudo-wave-functions in the context of pseudopotential constructions (see, e.g., Refs. 42 and 43). In view of the remaining very small differences concerning eigenvalues and eigenfunctions we considered it not worthwhile to construct and tabulate the ionic contributions $V_{ps,\alpha}$ to our pseudopotentials for each material *anew* but we employ, instead, the usual LDA pseudopotentials $V_{ps,\alpha}^{LDA}$ that are readily available from the literature.^{42,43} The close agreement of the resulting energies $\tilde{\epsilon}_{ps,\alpha}^{SIC-PP}$ with $\tilde{\epsilon}_{all-el}^{SIC-LDA}$ in Table I furthermore shows that the influence of SIC on the charge densities of deeper core states (e.g., Zn 3*s* and Zn 3*p* or Cd 4*s* and Cd 4*p*) can only affect the pseudopotentials for the semicore *d* electrons and the valence electrons of II-VI compounds marginally.

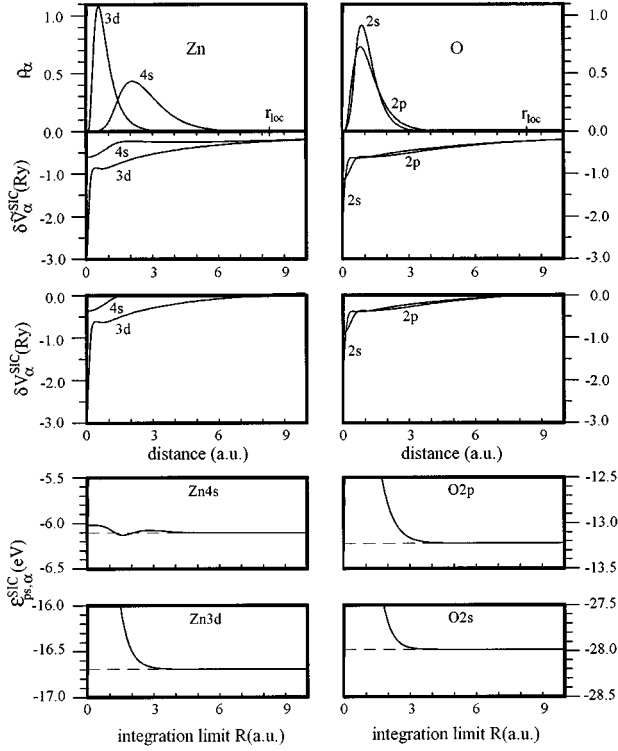


FIG. 3. Radial charge density distributions $\rho_\alpha(r) = 4\pi r^2 R_\alpha^2(r)$ for the Zn and O atoms (top panels) as resulting for the SIC-PPs including $\delta\tilde{V}_\alpha^{\text{SIC}}$. The latter are shown in the lower parts of the upper panels. The SIC-PP contributions $\delta V_\alpha^{\text{SIC}}$ according to Eq. (10) used in the solid-state calculations are shown in the middle panels. The lower panels show the expectation values $\varepsilon_{\text{ps},\alpha}^{\text{SIC}}(R)$ as defined in Eq. (12) for the Zn $4s$, Zn $3d$, O $2p$, and O $2s$ states as a function of the upper limit R of the r integration. They are converged to better than 0.5% for $R=3$ a.u. (see also Table II). Note that $\varepsilon_{\text{ps},\alpha}^{\text{SIC}}(R)$ in the lower panels is the expectation value of the full Hamiltonian according to Eq. (12).

This is different for Ge $3d$ core states. The SIC influence on their charge density has an appreciable effect on the resulting pseudopotential for the valence electrons, as has been shown in detail by Rieger and Vogl.³⁴ One should note in this context, that, e.g., Cd $4p$ and Cd $4s$ core states reside at -67 and -106 eV, respectively, while the Ge $3d$ core states reside at about -30 eV, only. In consequence, the SIC influence on the charge density of the latter has a much more noticeable effect on the respective pseudopotential for the valence electrons. Furthermore, we note that the $3d$ and $4d$ states in Zn and Cd, respectively, are in a sense equivalent to the $3d$ states in Ge. For these semicore d states we actually construct SIC-PPs so that the SIC effects on these d states are explicitly taken into account in our approach as well. It is obvious from Table I that SIC pseudopotentials yield a much better description of pseudoatoms than standard pseudopotentials $V_{\text{ps},\alpha}^{\text{LDA}}$ alone.

The SIC pseudopotentials $\tilde{V}_{\text{ps},\alpha}^{\text{SIC}}$ cannot directly be transferred to solid-state calculations because they all have the same asymptotic $-2/r$ tails arising from the Coulomb potential in $\delta\tilde{V}_\alpha^{\text{SIC}}$. This long-range behavior would cause an unwanted overlap between the SIC contributions from different atomic sites in the solid. But this overlap can easily be

avoided, as we will explicitly show for ZnO. We have chosen ZnO as a prototype example for our discussion because the shortcomings of the LDA approach using standard pseudopotentials are most pronounced for this compound. It is obvious from Fig. 3 that the atomic charge densities of the involved orbitals are strongly localized in space. In consequence, the long-range $-2/r$ tails of the potentials have no observable influence on the related atomic eigenvalues and eigenfunctions. *Actually, it is the product $V_{\text{Coul}}[n_\alpha^{\text{at}}]\Phi_\alpha^{\text{ps}}$ that matters in Eq. (5).* It vanishes when the related wave function vanishes. We can therefore simply define an appropriate radius r_{loc} beyond which the actual form of the SIC contribution to the atomic pseudopotential is insignificant for the eigenvalues and eigenfunctions of the pseudoatoms. We determine r_{loc} by the condition that the following restricted expectation value of the SIC contribution to the eigenvalues:

$$\int_0^{r_{\text{loc}}} \int_\Omega \Phi_\alpha^{\text{ps}}(\mathbf{r}) \delta\tilde{V}_\alpha^{\text{SIC}}(\mathbf{r}) \Phi_\alpha^{\text{ps}}(\mathbf{r}) r^2 dr d\Omega =: \delta\varepsilon_{\text{ps},\alpha}^{\text{SIC}}(r_{\text{loc}}), \quad (8)$$

has converged to within 10^{-3} eV for the most extended valence state involved in a compound. For the other less extended states convergence is then even better. We obtain $r_{\text{loc}}=8.34$ a.u. for the Zn and $r_{\text{loc}}=9.09$ a.u. for the Cd compounds using Zn $4s$ and Cd $5s$ orbitals in Eq. (8), respectively.

As is obvious from Fig. 3, the relevant products $\delta\tilde{V}_\alpha^{\text{SIC}}\Phi_\alpha^{\text{ps}}$ are of very short range except for the most extended orbital (Zn $4s$ in the example of Fig. 3). The latter product becomes short ranged, as well, if we make use at this point of the freedom to define the zero of our energy scale for the solid-state calculations. We can simply add on both sides of Eq. (5) the very same constant $2/r_{\text{loc}}$ (in Ry units) for all α . This merely redefines the zero of our energy scale, which is arbitrary in a solid-state calculation, anyway. The Kohn-Sham equations then read

$$\left\{ -\nabla^2 + V_{\text{ps},\alpha}^{\text{LDA}} + \delta\tilde{V}_\alpha^{\text{SIC}} + \frac{2}{r_{\text{loc}}} + V_{\text{Coul}}[n_v] + V_{\text{xc}}^{\text{LDA}}[n_v] \right\} \Phi_\alpha^{\text{ps}} = \left\{ \varepsilon_{\text{ps},\alpha}^{\text{SIC}} + \frac{2}{r_{\text{loc}}} \right\} \Phi_\alpha^{\text{ps}} =: \varepsilon_{\text{ps},\alpha}^{\text{SIC}} \Phi_\alpha^{\text{ps}}. \quad (9)$$

Since the $-2/r$ tails in $\delta\tilde{V}_\alpha^{\text{SIC}}$ are irrelevant beyond r_{loc} for the eigenvalues and eigenfunctions, we can now cut off the potentials at r_{loc} without sacrifice in accuracy. Our final SIC-PPs for the solid-state calculations are then given as

$$V_{\text{ps},\alpha}^{\text{SIC}} := V_{\text{ps},\alpha}^{\text{LDA}} + \delta V_\alpha^{\text{SIC}} := V_{\text{ps},\alpha}^{\text{LDA}} + \begin{cases} -V_{\text{Coul}}[n_\alpha^{\text{at}}] - V_{\text{xc}}^{\text{LSD}}[n_\alpha^{\text{at}}, 0] + \frac{2}{r_{\text{loc}}}, & r \leq r_{\text{loc}} \\ 0, & r > r_{\text{loc}} \end{cases} \quad (10)$$

so that we finally have to solve the following Kohn-Sham equations for the solids:

TABLE II. Results of a convergence study of the atomic term values of Zn and O resulting with our SIC-PPs as a function of the upper limit R of the r integration in Eq. (12). The values for $R = \infty$ exactly agree with the term values $\varepsilon_{\text{LDA}}^{\text{SIC-PP}}$ in Table I, except for the rigid shift of all levels by $2/r_{\text{loc}} \triangleq 3.26$ eV. The term-value *differences* which are relevant for the solid-state calculations, only, are not at all affected by this shift.

R (a.u.)	$\varepsilon_{\text{ps,Zn } 4s}^{\text{SIC}}$ (eV)	$\varepsilon_{\text{ps,O } 2p}^{\text{SIC}}$ (eV)	$\varepsilon_{\text{ps,Zn } 3d}^{\text{SIC}}$ (eV)	$\varepsilon_{\text{ps,O } 2s}^{\text{SIC}}$ (eV)
2	-6.11	-12.80	-16.52	-27.65
3	-6.08	-13.16	-16.68	-27.96
4	-6.10	-13.22	-16.70	-27.98
5	-6.11	-13.23	-16.70	-27.98
∞	-6.11	-13.23	-16.70	-27.98

$$\begin{aligned} & \{ -\nabla^2 + V_{\text{ps},\alpha}^{\text{SIC}} + V_{\text{Coul}}[n_v] + V_{\text{xc}}^{\text{LDA}}[n_v] \} \Phi_{\alpha}^{\text{ps}} \\ & = \varepsilon_{\text{ps},\alpha}^{\text{SIC}} \Phi_{\alpha}^{\text{ps}}. \end{aligned} \quad (11)$$

The SIC contributions $\delta V_{\alpha}^{\text{SIC}}$ to the SIC pseudopotentials are shown in Fig. 3 as well. Actually, by adding $2/r_{\text{loc}}$ on both sides of Eq. (9) we refer our energies to the flat plateau of $\delta \tilde{V}_{\alpha}^{\text{SIC}}$ for the Zn 4s (see Fig. 3) or Cd 5s states, respectively, i.e., to the flat plateau in the SIC contribution to the pseudopotential of the most extended state. In consequence, the product $\delta V_{\alpha}^{\text{SIC}} \Phi_{\alpha}^{\text{ps}}$ is now of extremely short range for the Zn 4s state as well (see Fig. 3). The fact that our pseudopotentials have a discontinuous slope at r_{loc} has no influence at all since the products $\delta V_{\alpha}^{\text{SIC}} \Phi_{\alpha}^{\text{ps}}$ vanish at r_{loc} . In this way we obtain a SIC pseudopotential which gives rise to only a truly short-ranged SIC contribution so that overlap effects of the SIC contributions become insignificant in the solid. The pseudopotentials $V_{\text{ps},\alpha}^{\text{SIC}}$ reproduce the differences between the term values as resulting with $\tilde{V}_{\text{ps},\alpha}^{\text{SIC}}$ from Eq. (5) within 10^{-3} eV and the related eigenfunctions are identical. It is important to recognize that the *atomic* pseudocharge densities n_{α}^{at} which are nearly identical to the solid-state pseudocharge densities in the II-VI compounds considered in this work enter the definition of our SIC-PPs in Eq. (10).

In order to identify the spatial region around each atom which contributes to the SIC part of the eigenvalues, we have calculated

$$\begin{aligned} \varepsilon_{\text{ps},\alpha}^{\text{SIC}}(R) & := \langle \Phi_{\alpha}^{\text{ps}} | \hat{H}_{\text{eff},\alpha}^{\text{LDA}} | \Phi_{\alpha}^{\text{ps}} \rangle \\ & + \int_0^R \int_{\Omega} \Phi_{\alpha}^{\text{ps}}(\mathbf{r}) \delta V_{\alpha}^{\text{SIC}}(\mathbf{r}) \Phi_{\alpha}^{\text{ps}}(\mathbf{r}) r^2 dr d\Omega \end{aligned} \quad (12)$$

as a function of the upper limit R of the r integration. The resulting functions $\varepsilon_{\text{ps},\alpha}^{\text{SIC}}(R)$ are shown in the lower panels of Fig. 3 for the Zn 4s, Zn 3d, O 2p, and O 2s states and some respective energies are given in Table II for a number of R values. It is obvious from Fig. 3 and Table II that the SIC contributions converge very fast as a function of R . As a matter of fact they have converged already to better than 1% at $R=2$ a.u. for the different states except for O 2p for which this convergence level is reached at $R=2.6$ a.u. This

TABLE III. Relaxation-induced atomic energy shifts $\delta \tilde{V}_{\alpha}^{\Delta\text{SCF}}$ (in eV) to the pseudopotentials according to Eq. (14) as given by the respective differences between atomic ΔSCF binding energies and LDA term values calculated employing our SIC-PPs. Note that these values are no free parameters but they are uniquely determined from the respective calculations and can directly be read off from Table I. The values resulting for Zn 4s and Cd 5s from Table I are put in parentheses. Their use would mean fully incorporating the electronic relaxation of atomic Zn 4s and Cd 5s states. Because it is more meaningful to ignore the ΔSCF shifts of these conduction-band states altogether in the respective SIRC-PPs (for details, see text) we neglect the respective shifts in our optimal SIRC pseudopotentials, setting them to zero.

	Zn 4s	Zn 3d	Cd 5s	Cd 4d	O 2s	O 2p
$\delta \tilde{V}_{\alpha}^{\Delta\text{SCF}}$	0.0		0.0			
	(-0.5)	2.1	(-0.5)	0.7	0.3	0.3
	S 3s	S 3p	Se 4s	Se 4p	Te 5s	Te 5p
$\delta \tilde{V}_{\alpha}^{\Delta\text{SCF}}$	0.1	-0.2	0.0	-0.3	-0.2	-0.4

proves that the SIC contributions to the eigenvalues originate from an extremely short-ranged region around each atom.

2. Self-interaction and relaxation-corrected pseudopotentials

So far, we have incorporated dominant self-interaction corrections in our SIC pseudopotentials but we have not yet sufficiently accounted for *electronic relaxation*. For the sake of brevity, we will refer to our pseudopotentials incorporating self-interaction corrections and electronic relaxation as *self-interaction and relaxation-corrected* (SIRC) pseudopotentials. When electronic band structures are measured, e.g., by angle-resolved photoelectron spectroscopy (ARPES), electrons are excited from occupied states. The lower these states reside in energy below the Fermi level and the more they are localized in space, the larger is the relaxation of the valence-electron system in response to the excitation. This relaxation gives rise to shifts in energy of the experimentally observable levels. This was clearly to be seen already in the results for atoms (see Table I) as we have discussed in Sec. II A. The all-electron ΔSCF binding energies show significant shifts with respect to the all-electron SIC-LSD or SIC-LDA eigenvalues. The shifts are most pronounced for highly localized semicore d states, as we have pointed out already. Our SIC-PPs were constructed in Sec. II B 1 such that they yield basically the same eigenvalues and eigenfunctions for the pseudoatoms as the full SIC-LSD or SIC-LDA formalism of Perdew and Zunger.²³ In consequence, they naturally cannot yield a better description of the semicore d states than the full SIC calculations. Therefore an accurate description of d -band positions, in particular, can only be achieved if more accurate *atomic* binding energies are built into the construction of appropriate pseudopotentials from the start. This can indeed be achieved by referring to the ΔSCF results for the constituent atoms, as given in Table I. An improvement of the d -band description in the solid is to be expected if we devise our pseudopotentials such that they yield the *atomic* ΔSCF binding energies exactly. To this end we make use of the freedom to construct our pseudopotentials accordingly.

In the construction of our SIRC-PPs we follow the same general route as for the SIC-PPs in Sec. II B 1. We define SIRC pseudopotentials for *atoms* as

$$\tilde{V}_{ps,\alpha}^{\text{SIRC}} := \tilde{V}_{ps,\alpha}^{\text{SIC}} + \delta\tilde{V}_{\alpha}^{\Delta\text{SCF}}. \quad (13)$$

The relaxation-induced shifts $\delta\tilde{V}_{\alpha}^{\Delta\text{SCF}}$ are defined such that the SIRC-PPs yield atomic eigenvalues which exactly equal the ΔSCF binding energies. This is simply accomplished by defining

$$\delta\tilde{V}_{\alpha}^{\Delta\text{SCF}} := E_{\alpha}^{\text{LDA-}\Delta\text{SCF}} - \tilde{\epsilon}_{\alpha}^{\text{SIC-PP}}. \quad (14)$$

The values $\delta\tilde{V}_{\alpha}^{\Delta\text{SCF}}$ can simply be read off from Table I and they are compiled for the convenience of the reader in Table III. Note that they are no free parameters but are uniquely determined from the *calculated differences* between $E_{\alpha}^{\text{LDA-}\Delta\text{SCF}}$ and $\tilde{\epsilon}_{\alpha}^{\text{SIC-PP}}$. The SIRC pseudopotentials are then transferred to the solid and, to avoid unwanted overlap effects, they are cut off in the same way as the SIC-PPs were cut off in Sec. II B 1. They are then explicitly given as

$$V_{ps,\alpha}^{\text{SIRC}} := V_{ps,\alpha}^{\text{SIC}} + \delta V_{\alpha}^{\Delta\text{SCF}} := V_{ps,\alpha}^{\text{LDA}} + \begin{cases} -V_{\text{Coul}}[n_{\alpha}^{\text{at}}] - V_{\text{xc}}^{\text{LDS}}[n_{\alpha}^{\text{at}}, 0] + \frac{2}{r_{\alpha}}, & r \leq r_{\alpha} \\ 0, & r > r_{\alpha}. \end{cases} \quad (15)$$

The cutoff radii follow from Eqs. (10) and (15) as

$$\frac{2}{r_{\alpha}} = \delta\tilde{V}_{\alpha}^{\Delta\text{SCF}} + \frac{2}{r_{\text{loc}}}. \quad (16)$$

Note that the $\delta V_{\alpha}^{\Delta\text{SCF}}$ in Eq. (15) have a small space-dependent contribution while the $\delta\tilde{V}_{\alpha}^{\Delta\text{SCF}}$, defined in Eq. (14), are constants. The respective energy shifts $2/r_{\alpha}$ (in a.u.) guarantee that the $V_{ps,\alpha}^{\text{SIRC}}$ exactly reproduce the atomic ΔSCF binding energies when used in a standard LDA calculation. We employ our atomic LDA- ΔSCF energies instead of the SIC-LDA- ΔSCF energies in this construction because the former are in slightly better agreement with experiment than the latter.

The terms $\delta V_{\alpha}^{\Delta\text{SCF}}$ entering the nonlocal short-range part of our pseudopotentials are orbital dependent. This is perfectly alright since electronic relaxation is different for different orbitals. So it can only be taken into account appropriately in an effective one-particle potential by orbital-dependent contributions. This is in the same spirit as standard pseudopotential theory which describes the scattering properties of atomic potentials by different angular-momentum-dependent components for different orbitals in the respective nonlocal short-range parts of $V_{ps,\alpha}^{\text{LDA}}$. The nonlocal relaxation-induced contributions in our SIRC-PPs are again extremely short ranged. By construction, they yield nearly the same wave functions as our SIC-PPs and atomic eigenvalues which exactly equal the atomic ΔSCF binding energies.

There is one final point to be considered in the context of the SIRC-PPs. In Eq. (14) we have fully incorporated electronic relaxation as it applies to the constituent atoms of the considered compounds and we have transferred these poten-

tials in Eq. (15) to the solids. But employing the relaxation-induced ΔSCF shifts of the *atomic* Zn 4*s* and Cd 5*s* states in a solid-state calculation is certainly not fully appropriate. In Zn and Cd atoms the 4*s* and 5*s* subshells are fully occupied by two electrons but in Zn and Cd *compounds* the Zn 4*s* and Cd 5*s* states form the bottom of the conduction bands and they are not fully occupied, therefore. From a Mullikan analysis of orbital occupancies⁴¹ we find that the Zn 4*s* states of, e.g., ZnO are only occupied by 0.52*e* and the Cd 5*s* states of, e.g., CdS are only occupied by 0.71*e*, clearly evidencing the large ionicity of these compounds. It would thus not be quite correct to fully implement the relaxation-induced shifts $\delta\tilde{V}_{\alpha}^{\Delta\text{SCF}}$ of the *atomic* Zn 4*s* and Cd 5*s* states in the construction of the respective 4*s* and 5*s* pseudopotentials of the solid. The limiting alternative is to ignore the relaxation-induced shifts $\delta\tilde{V}_{\alpha}^{\Delta\text{SCF}}$ in the Zn 4*s* and Cd 5*s* SIRC pseudopotentials for the solids altogether. Certainly, the truth lies somewhere in between applying full atomic relaxation and entirely neglecting it. But the truth is certainly closer to the neglect of electronic relaxation of the Zn 4*s* and Cd 5*s* states than fully incorporating it, as is obvious from the orbital occupancies in the solids. Which one of the two variants is more appropriate can eventually only be decided on the basis of actual results. It turns out that the entire neglect of the $\delta\tilde{V}_{\alpha}^{\Delta\text{SCF}}$ shifts for Zn 4*s* and Cd 5*s* states overall yields considerably better results than applying full relaxation to these states, as was to be expected in view of the relatively small orbital occupancies of these orbitals in the solids. Thus our optimal SIRC-PPs are defined as in Eqs. (15) and (16) with the respective $\delta\tilde{V}_{\alpha}^{\Delta\text{SCF}}$ values as given in Table III.

This concludes the construction of our pseudopotentials for II-IV compounds. They are defined in Eqs. (10) and (15), respectively. According to the general arguments detailed in this section we expect our SIC-PPs to yield a considerably better description of electronic properties of II-VI semiconductor compounds than standard pseudopotentials $V_{ps,\alpha}^{\text{LDA}}$ and the SIRC-PPs to yield the best description as far as agreement with measured electronic properties is concerned.

3. Implementation of the pseudopotentials

The pseudopotentials $V_{ps,\alpha}^{\text{SIC}}$ and $V_{ps,\alpha}^{\text{SIRC}}$ can now be separated, as usual, into a local long-range and an orbital-dependent short-range part. According to Eqs. (10) and (15) the long-range parts of these potentials are identical to the long-range part of $V_{ps,\alpha}^{\text{LDA}}$ and thus have the usual asymptotic $-2Z_v/r$ behavior. This long-range part is treated as a local potential in the calculations for the solid, as usual. The nonlocal parts of $V_{ps,\alpha}^{\text{SIC}}$ or $V_{ps,\alpha}^{\text{SIRC}}$ consist of the nonlocal part of $V_{ps,\alpha}^{\text{LDA}}$ and the nonlocal, short-range SIC or SIC- ΔSCF contribution $\delta V_{\alpha}^{\text{SIC}}$ or $\delta V_{\alpha}^{\text{SIC}} + \delta V_{\alpha}^{\Delta\text{SCF}}$, respectively. These potentials now have the standard form of nonlocal, norm-conserving pseudopotentials but they have built in the most dominant self-interaction corrections or self-interaction and relaxation corrections, respectively, that need to be accounted for in more accurate solid-state electronic structure calculations. They can simply be transformed into the separable form as suggested by Kleinman and Bylander⁴⁴ (see the Appendix) and can directly be implemented in a solid-state LDA band-structure calculation. Therefore, simplified SIC-LDA or SIC-LDA- ΔSCF calculations for solids can be carried out by employing our SIC-PPs or our SIRC-PPs using a

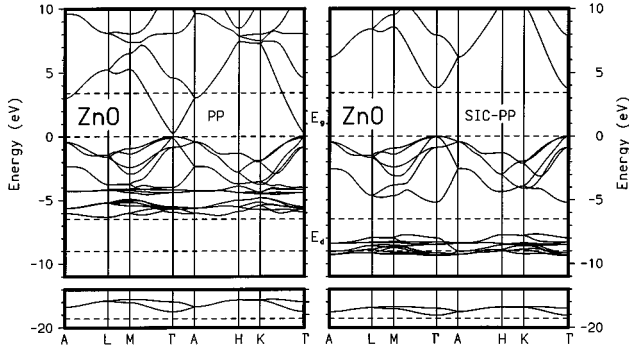


FIG. 4. LDA bulk band structure of ZnO as calculated using standard pseudopotentials (PP, left panel) or our SIC pseudopotentials (SIC-PP, right panel). All energies are referred to the respective top of the valence bands. The horizontal dashed lines indicate the measured gap energy (from Ref. 48), the d -band width (from Ref. 16), and the anion s -band width (from Ref. 13).

standard LDA band-structure code. Only the input pseudopotentials need to be changed according to Eqs. (10) or (15), respectively, at the very beginning of the self-consistent iterations. In consequence, our approximate approach is very efficient and can easily be transferred to more complicated systems such as surfaces or interfaces. We have carried out such calculations employing our pseudopotentials for ZnO(10 $\bar{1}0$), CdS(10 $\bar{1}0$), and CdSe(10 $\bar{1}0$) surfaces. A preliminary account of results for surfaces, which will be discussed in detail elsewhere, is given in Ref. 45. The results show very good agreement with experiment, indeed.

III. RESULTS

In this section we present and discuss results of applications of our pseudopotentials in electronic structure calculations for bulk II-VI compound semiconductors. All these calculations were carried out at the experimental lattice constants. We have studied 11 zinc-blende (ZB), wurtzite (W), and rocksalt (RS) structures of Zn and Cd compounds. Most of these structures are stable under normal conditions but some can only be grown epitaxially on suitable substrates. For each of the 11 configurations we have carried out four separate self-consistent LDA calculations employing standard pseudopotentials V^{LDA} , our SIC pseudopotentials V^{SIC} , and the two variants of our SIRC pseudopotentials V^{SIRC} . To identify the influence of the relaxation-induced shifts $\delta\bar{V}_\alpha^{\text{ASCF}}$, as discussed in Sec. II B 2, we have carried out two SIRC-PP calculations for each material using for the Zn $4s$ and Cd $5s$ components either the full atomic relaxation shift (-0.5 eV, as shown in parentheses in Table III) or entirely neglecting it in the SIRC-PPs. Therefore we have in total 44 band structures of II-VI compounds available as a data basis for an identification of the applicability and usefulness of our pseudopotentials. As is obvious from Eqs. (10) and (15) the standard pseudopotentials V^{LDA} enter in all our calculations. We employ the ionic pseudopotentials of Bachelet, Hamann, and Schlüter⁴² for the Zn and Cd cations and those of Gonze, Stumpf, and Scheffler⁴³ for the O, S, Se, and Te anions. In all our calculations the exchange-correlation potential is taken into account in the Ceperley-

Alder form⁴⁶ as parametrized by Perdew and Zunger.²³ For the selenides and tellurides we have taken spin-orbit coupling into account, in addition. As basis sets we employ 80 Gaussian orbitals per unit cell for the RS and ZB and 160 Gaussian orbitals per unit cell for the W compounds, respectively, with appropriately determined decay constants. Brillouin-zone sums are carried out at six and ten special \mathbf{k} points⁴⁷ for the W and RS or ZB crystals, respectively.

A. Result obtained using V^{SIC}

Let us first address the band structure of ZnO which shows the most severe shortcomings as compared to experiment when it is calculated with standard pseudopotentials. The full bulk band structure of ZnO is shown along the high-symmetry lines of the hexagonal Brillouin zone in Fig. 4. The left panel shows the standard PP and the right panel shows the SIC-PP result. The measured gap, d -band width, and anion s -band position are indicated by horizontal dashed lines in each case. Both band structures exhibit four band groups that are characteristic for W II-VI compounds. The lowest two bands derive from anion s states (O $2s$). Next follow the ten cationic semicore d bands (Zn $3d$) and closely above these reside the six mostly anion-derived O $2p$ valence bands. Above the gap we observe the lowest group of conduction bands, the bottom of which is mostly derived from cationic s states (Zn $4s$). All shortcomings of standard pseudopotential LDA calculations mentioned already in the Introduction are most obvious in the left panel of Fig. 4. The O $2p$ valence bands occur close to the conduction bands. The semi-core d bands occur roughly 3 eV too high in energy as compared to experiment. In consequence their interaction with the anion p valence bands (mainly O $2p$ derived) is unrealistically strong. The dispersion of these p bands is therefore falsified. More importantly, they are pushed up in energy close to the bottom of the conduction bands so that the fundamental gap is almost closed. All these deficiencies are overcome to a large extent by employing our SIC-PPs, as is obvious from the right panel of Fig. 4. The Zn $3d$ bands and the O $2p$ bands now occur considerably lower in energy relative to the bottom of the conduction bands. Concomitantly, the O $2p$ valence bands are no longer pushed up very close to the conduction-band bottom and the p - d interactions are much smaller now. In consequence, the gap has opened up dramatically and the width of the O $2p$ valence bands has increased from 4.0 eV (left panel) to 5.2 eV (right panel). The results of our SIC-PP calculations are in much better agreement with experiment than the standard PP results, as is obvious from the right panel of Fig. 4. The calculated O $2p$ valence-band width of 5.2 eV, in addition, agrees remarkably well with the measured bandwidth of 5.3 eV.⁴⁸ It is important to note that our SIC-PPs not only give rise to rigid shifts of entire band groups but they also influence the dispersion, most noticeably of the occupied bands, considerably. This is the case because reduced p - d interactions and the respectively increased s - d interactions alter the dispersions of all occupied bands to some extent. In addition, our SIC-PPs have space-dependent contributions $\delta V^{\text{SIC}}(\mathbf{r})$ that considerably affect the dispersions as well.⁴⁹ In summary, we observe impressive improvements in the band structure of ZnO resulting from a straightforward implementation of our SIC-PPs within standard LDA calculations.

TABLE IV. Gap energies E_g and average d -band energies E_d (in eV) as resulting from LDA calculations employing standard PPs, SIC-PPs, and SIRC-PPs, respectively, in comparison with experimental data from Ref. 48, if not stated otherwise. Note that the d bands have a considerable width both in experiment and in theory (see, e.g., Figs. 4, 8, and 9). We give average d -band energies as resulting from our calculations while experiment usually cites the energetic position of the maximum of the d -band peak.

		PP	SIC-PP	SIRC-PP	Expt.
ZnO ^w	E_g	0.2	3.8	3.5	3.4
	E_d	-5.0	-8.9	-7.5	-7.8
ZnS ^w	E_g	2.0	3.4	3.7	3.9
	E_d	-5.9	-11.4	-9.4	
ZnS ^{ZB}	E_g	1.8	3.3	3.6	3.7 ^a
	E_d	-5.7	-11.4	-9.5	-9.0
ZnSe ^{ZB}	E_g	0.6	1.8	2.1	2.7 ^a
	E_d	-6.2	-12.2	-10.1	-9.4
ZnTe ^{ZB}	E_g	0.7	1.0	1.4	2.4
	E_d	-6.5	-13.0	-10.8	-9.8
CdO ^{RS}	E_g	-0.6	2.0	1.7	0.8
	E_d	-6.2	-9.0	-8.2	-12.0
CdS ^w	E_g	1.2	2.4	2.5	2.5 ^b
	E_d	-6.8	-10.5	-9.7	-9.6
CdS ^{ZB}	E_g	1.1	2.2	2.4	2.4 ^a
	E_d	-6.8	-10.5	-9.7	
CdSe ^w	E_g	0.4	1.1	1.4	1.8
	E_d	-7.4	-11.3	-10.4	-10.0
CdSe ^{ZB}	E_g	0.2	1.1	1.3	
	E_d	-7.4	-11.3	-10.4	
CdTe ^{ZB}	E_g	0.3	0.5	0.8	1.6
	E_d	-7.8	-12.2	-11.0	-10.5

^aReference 50.

^bReference 51.

Let us now broaden the data base for a more general discussion of the effects brought about in the band structures of II-VI compounds by the SIC-PPs. We first concentrate on salient key features, namely, the gap and the d -band energies. They are given in Table IV, as resulting for the different pseudopotentials used, together with experimental data.^{48,50,51} Obviously in all cases the results obtained with standard pseudopotentials^{42,43} are largely at variance with the experimental data. Our SIC-PP results, in general, grossly improve the agreement between theory and experiment.

Comparing the PP and SIC-PP results in the first two columns of Table IV we may discern *primary* and *secondary* effects of the SIC contribution to the pseudopotentials. The most pronounced primary effect is that the SIC-PPs induce shifts of the band groups in the solids that are very similar in nature to the respective SIC-induced shifts of the related atomic term values (cf. Table I and Fig. 2). We observe that the cationic d bands strongly shift to lower energies with respect to the anionic p valence bands. Comparing the d -band energies as resulting from PP and SIC-PP calculations, they occur roughly 6 eV lower in energy for the Zn compounds, except for ZnO where they are only lowered by 4 eV, and they occur some 4 eV lower in energy for the Cd compounds, except for CdO where the related shift is about 3 eV. The somewhat different behavior of the compounds in-

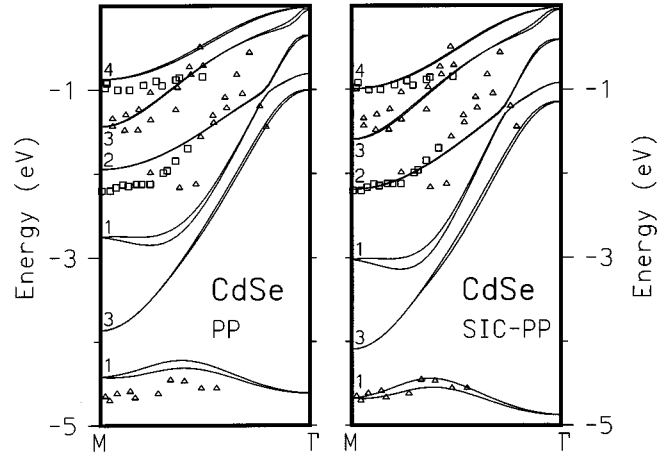


FIG. 5. Comparison of calculated and measured upper valence bands of W CdSe. The LDA band structures have been calculated with standard pseudopotentials (PP, left panel) and with our SIC pseudopotentials (SIC-PP, right panel). Spin-orbit coupling has explicitly been taken into account. The symmetry of the calculated bands (1, 3 even and 2, 4 odd with respect to the mirror plane) favorably compares with the polarization and angle-resolved photoelectron spectroscopy data (Δ even and \square odd, from Ref. 52).

volving O is related to the fact that the highly localized O $2s$ and O $2p$ orbitals show a much stronger SIC effect than the comparatively more extended s and p orbitals of S, Se, and Te. In consequence the SIC shift of the cation d bands relative to the anion p bands is smaller in ZnO and CdO than in the other compounds. The energetic lowering of semicore d bands is more pronounced in Zn compounds (roughly 6 eV) than in Cd compounds (roughly 4 eV), as was to be expected. The respective atomic term values (cf. Table I and Fig. 2) show the same behavior, which is simply due to the fact that Zn $3d$ states are more localized than Cd $4d$ states and therefore show a larger SIC shift.

Another very gratifying primary effect is the downward shift of the anion p valence bands relative to the cation s conduction bands. There are two reasons for it. First, the anion p states are much more localized than the cation s states and therefore undergo a comparatively larger SIC shift (see also Fig. 2) and second, the p valence bands are no longer pushed up in energy by unrealistically large p - d interactions. In consequence, the gap opens up considerably in many of the compounds. This effect is most pronounced for compounds involving O and it decreases with increasing spatial extent of the anion p orbitals. In addition, it is more pronounced in the Zn than in the Cd compounds. This is due to the fact that the d bands occur already comparatively lower with respect to the anion p bands in the Cd than in the Zn compounds when they are calculated with standard pseudopotentials. Thus the reduction of p - d interactions due to the SIC-induced downward shift of the d bands is more pronounced in the latter than in the former. This general behavior nicely correlates with the related SIC-induced shifts in the atoms (cf. Table I and Fig. 2) and with the ionicity of the compounds. The more ionic a compound (e.g., ZnO or CdO) the more localized are its wave functions and the larger are the SIC effects. The relatively least ionic and most cova-

lent compounds in our series (i.e., ZnTe and CdTe) show the weakest SIC effects in their band structures.

As an important secondary effect, we observe changes in the dispersions of the shifted bands as mentioned already in the context of Fig. 4 for ZnO. Similar changes induced by $\delta V_{\alpha}^{\text{SIC}}(\mathbf{r})$ in the dispersions of anion-derived p valence bands are observed for other compounds as well. In Ref. 32 we have shown comparisons of calculated and measured bands for ZnO and for W CdS. Using our SIC-PPs, we obtained considerably improved agreement with the data of Zwicker and Jacobi¹⁶ for ZnO and of Magnusson and Flodström⁵² for W CdS, as compared to our standard LDA results, concerning both the dispersion and the symmetry properties of these bands. In Fig. 5 we show a respective comparison between calculated and measured bands for W CdSe. The agreement of our SIC-PP results with the data of Magnusson and Flodström⁵² is again very satisfactory. Not only the dispersions, in particular from M to $M\Gamma/2$, and the symmetry character of the calculated and measured bands are in good agreement but also the measured energy position and the spin-orbit splitting of the two bands near -5 eV are very well described by our SIC-PP results. The remaining deviations between calculated and measured bands closer to the Γ point could very well be related to experimental difficulties in precisely determining the intrinsic top of the valence bands with respect to the extrinsic Fermi level.⁵³ Similar deviations occur near the Γ point for W CdS, as well.³²

Another secondary effect is to be noted. In all compounds the downward shift of the semi-core d bands leads to an increased s - d interaction with the low-lying anionic s bands giving rise to a decrease of their dispersions. This effect is most pronounced in ZnS and CdS but it is also to be seen in Fig. 4 for ZnO.

In spite of all the improvements obvious from Table IV and Figs. 4 and 5 there still remain distinct deviations between our SIC-PP results and experiment, most noticeably concerning the gap energy and the *absolute* position of the d bands. The main goal of our SIC-PP calculations was to overcome the misplacement of the d bands and the related unphysical consequences on gap energies, as well as on p -band widths and dispersions which are characteristic for standard LDA results. That goal has been reached and from any practical point of view our effective LDA-type Hamiltonians employing SIC-PPs are already far superior, as compared to standard pseudopotential LDA Hamiltonians, for all applications mentioned in the Introduction. But now, as is obvious from the second column of Table IV, the d bands occur up to 3 eV too low in energy for the Zn compounds (except ZnO) and roughly 1 eV too low in energy for the Cd compounds (except CdO) as compared to experiment. For calculations of occupied bands near the gap energy region as needed, e.g., for comparisons with ARPES data, this is of no practical relevance. But it remains, nevertheless, a nuisance from a general theoretical point of view. As we have already discussed in the context of Table I and in Sec. II B 2, that problem is related to electronic relaxation, which is not properly accounted for in V^{SIC} .

B. Results obtained using V^{SIRC}

To address the remaining problems mentioned above, we have taken electronic relaxation into account as well, in the

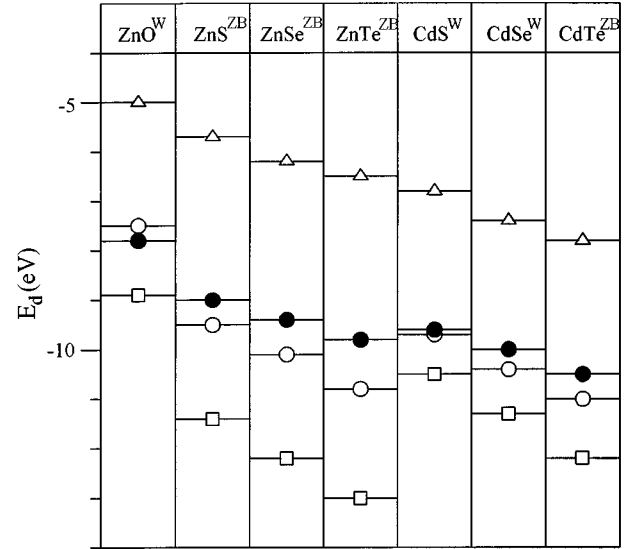


FIG. 6. Calculated average d -band positions for some II-VI compounds which are stable in W or ZB modification under normal conditions. Theoretical results are shown by open symbols while experimental data (from Ref. 48) are shown by full dots (\bullet). Our LDA calculations have been carried out with standard PPs (\triangle), SIC-PPs (\square), and with SIRC-PPs (\circ).

way described in Sec. II B 2. The respective SIRC-PP results are given in the third column of Table IV. The question whether one should fully incorporate the atomic ΔSCF shifts due to electronic relaxation in a solid-state calculation was addressed already in Sec. II B 2. This question is most relevant for the resulting gap energies. We have stated already that the complete neglect of atomic relaxation-induced shifts of the Zn $4s$ and Cd $5s$ states is probably more meaningful

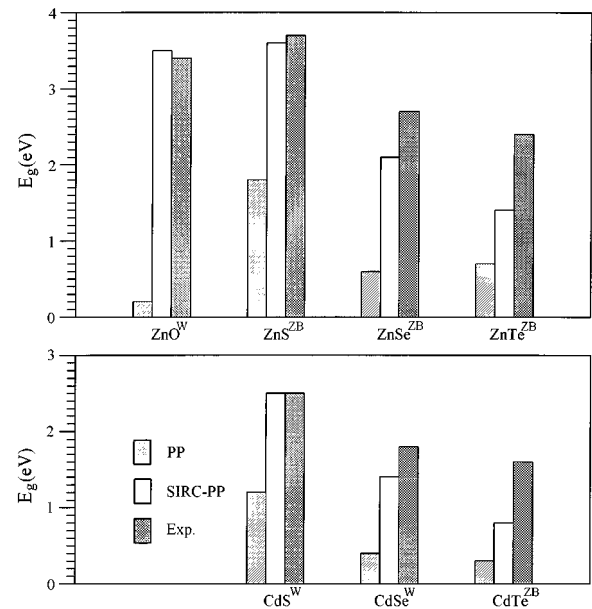


FIG. 7. Calculated and measured gap energies for some stable II-VI compounds. Our LDA values resulting with standard pseudopotentials (PP) and with our SIRC pseudopotentials (SIRC-PP) are compared with the experimental data from Refs. 48, 50, and 51.

TABLE V. Energy differences (in eV) between anion s and d term values of Zn and Cd atoms in comparison with the related energy differences between the bottom of the conduction bands E_c and the d -band positions in Zn and Cd compounds, given by $E_c - E_d$, as resulting with standard pseudopotentials (PP), SIC pseudopotentials (SIC-PP), and the two variants of our SIRC pseudopotentials (SIRC-PP). Our results for the SIRC-PPs including full atomic relaxation shifts are labeled by FR and those resulting for the SIRC-PPs neglecting relaxation of the anion s conduction-band states are labeled NR (for details, see text). Experimental data are from Refs. 48, 50, and 51.

	PP	SIC-PP	SIRC-PP ^{FR}	SIRC-PP ^{NR}	Expt.
$E_{\text{Zn } 4s} - E_{\text{Zn } 3d}$	4.2	10.6	8.0	8.5	7.8
$E_c - E_d$					
ZnO ^W	5.2	12.7	12.2	11.0	11.2
ZnS ^{ZB}	7.9	14.7	12.0	13.1	12.7
ZnSe ^{ZB}	7.5	14.0	11.3	12.2	12.3
ZnTe ^{ZB}	6.8	14.0	11.4	12.2	12.2
$E_{\text{Cd } 5s} - E_{\text{Cd } 4d}$	5.9	9.8	8.6	9.1	8.6
$E_c - E_d$					
CdS ^W	8.0	12.9	11.6	12.2	12.1
CdSe ^{ZB}	7.8	12.4	11.2	11.8	11.8
CdTe ^{ZB}	8.1	12.7	11.3	11.8	12.3

than fully incorporating it. This conclusion is borne out by our SIRC-PP results. Fully incorporating the $\delta\tilde{V}_\alpha^{\text{ASCF}}$ shifts of all atomic states in our potentials for the solids, indeed, yields d -band energies that agree with experiment within 0.5–0.8 eV but the gap energies are less accurate than in the results obtained neglecting the $\delta\tilde{V}_\alpha^{\text{ASCF}}$ contributions to the Zn 4s and Cd 5s pseudopotentials. Our final results, given in the third column of Table IV, were obtained with the latter SIRC-PPs.

In Fig. 6 we show a direct comparison of d -band positions as resulting from PP, SIC-PP, and SIRC-PP calculations with experimental data for seven ZB and W compounds. These seven compounds are stable under normal conditions. The underbinding of the d bands by roughly 3 eV in standard PP calculations and their overbinding in SIC-PP calculations is clearly to be seen. The SIRC pseudopotentials, on the contrary, yield d -band energies in reasonable agreement with experiment. The deviations are less than or equal to 0.5 eV except for the ZB compounds ZnSe and ZnTe where the remaining differences are 0.7 and 1.0 eV, respectively.

In Fig. 7 we show a direct comparison of measured gap energies with respective PP and SIRC-PP results. It is most obvious from Table IV and Figs. 6 and 7 that the SIRC pseudopotentials not only yield very satisfactory d -band positions from any practical point of view but also significantly improved results for the gap energies, in particular, for the more ionic compounds. Only with increasing covalent character of the binding and with increasing spatial extent of the anion p orbitals in the selenides and tellurides does the agreement decrease to some extent. This may be related to the stronger hybridization in these more covalent solids. Our approximation of calculating the SIC contributions to the

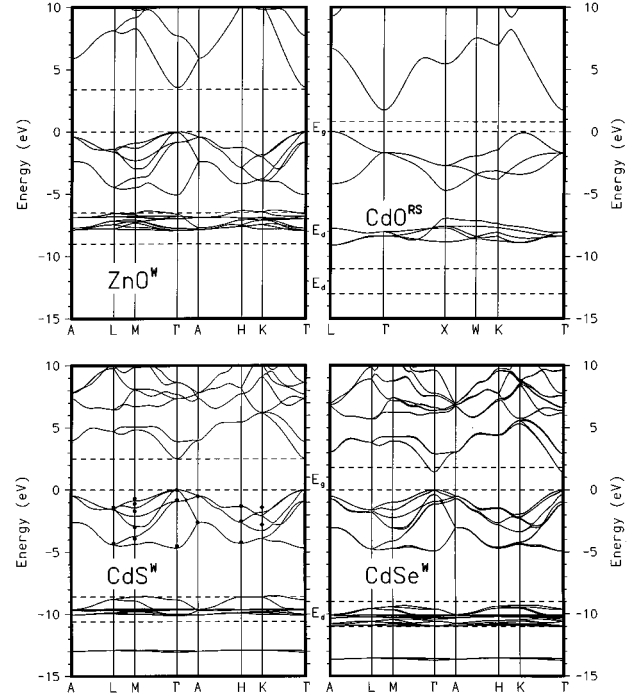


FIG. 8. LDA bulk band structures of wurtzite ZnO, CdS, CdSe, and of rocksalt CdO as resulting with our SIRC-PPs. All energies are referred to the respective top of the valence bands. The horizontal dashed lines indicate measured gap energies and d -band widths (from Refs. 16, 48, 50, and 51). In the band structure of W CdS (lower left panel) we have included ARPES data (heavy dots; from Ref. 55) at high-symmetry points for comparison.

pseudopotentials by employing atomic orbital-charge densities n_α^{at} certainly becomes less accurate in these compounds.

It is interesting to note that the gap energies in ZB ZnSe and ZnTe and W CdSe show precisely the same deviations from experiment as the respective d -band positions (see Table IV). The related deviations are similar for ZB CdTe as well. This shows that the *energy difference* between Zn 4s and Zn 3d or Cd 5s and Cd 4d states is accurately described in our calculations both in the atom and in the solids. Only the relative positions of the Se 4p and Te 5p bands deviate by 0.6, 1.0, 0.4, and 0.8 eV, respectively.⁵⁴ It is most revealing to address these *energy differences* as resulting from our calculations in some more detail. In Table V we have summarized the differences between anion s and d term values of the Zn and Cd pseudoatoms in comparison with the related energy differences $E_c - E_d$, where E_c is the bottom of the conduction bands. Since the bottom of the conduction bands in the II-VI compounds is derived from anion s states, the energy difference $E_c - E_d$ is a measure for the change of $E_s^{\text{cation}} - E_d^{\text{cation}}$ that occurs when Zn or Cd atoms are incorporated in Zn or Cd compounds. The respective changes in the solid, on the one hand, result from interactions, most importantly from first-nearest-neighbor anion-cation and second-nearest-neighbor cation-cation interactions. But in addition, the different electronic screening in the compounds as compared to that in the atoms gives rise to changes in these energy differences as well. First we note in Table V that the respective energy differences in the cations and in the compounds are significantly different. Our approach

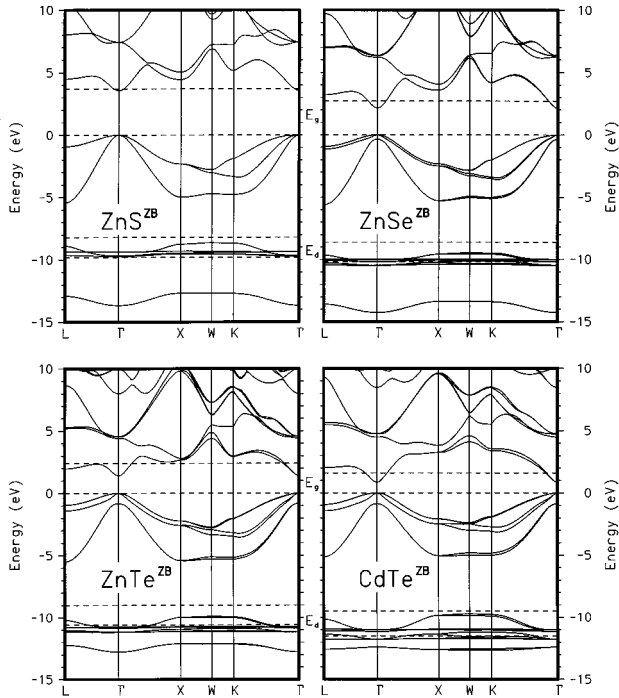


FIG. 9. LDA bulk band structures of zinc-blende ZnS, ZnSe, ZnTe, and CdTe as resulting with our SIRC-PPs (see also caption of Fig. 8).

yields this behavior appropriately, although we have only incorporated atomic properties of the constituent atoms in our pseudopotentials. This simply means that the use of our SIRC-PPs on a crystal lattice gives rise to a correct description of interactions and of electronic screening in the solids. Second we note that the standard PPs entirely fail to describe the measured differences accurately, both in the pseudoatoms and in the compounds, as was to be expected. Our SIC-PPs considerably improve on the comparison but there are still significant deviations from the measured energy differences. In the *pseudoatoms* our SIRC-PPs including full atomic relaxation yield the best agreement with the data, as was to be expected on the basis of their construction. But for the *solids* the SIRC-PPs including full relaxation yield energy differences which deviate up to 1.0 eV from the data. Our optimal SIRC-PPs, which entirely neglect the relaxation-induced shifts $\delta V_{\alpha}^{\Delta\text{SCF}}$ of Zn 4s and Cd 5s states in the solids, yield energy differences which are very close to the data (see the fourth and fifth columns of Table V), showing that these atomic SIRC-PPs and their appropriate transfer to the solids constitute a reliable basis for accurate band-structure calculations of II-VI compounds.

In Figs. 8 and 9 we show band structures for II-VI Zn and Cd compound semiconductors that are stable in RS, ZB, or *W* configurations, respectively, under normal conditions. Figure 8 shows our SIRC-PP results for *W* and RS compounds while Fig. 9 shows respective results for ZB compounds. We note again that the compounds containing Se and Te have been studied including spin-orbit interaction. We have indicated the measured fundamental gaps and *d*-band widths^{16,48,51,55} by horizontal dashed lines in each case. In all band structures we observe significant improvements, as compared to standard PP band structures, concern-

ing the comparison between theory and experiment except for the RS compound CdO. For this compound, the measured *d*-band position of -12 eV is much lower than the calculated average *d*-band position of -8.2 eV. The experimental result is somewhat astonishing in view of the fact that the measured *d*-band energy for CdO does not at all follow the trend in *d*-band positions that is obvious from Table IV and Fig. 6. The *d*-band binding energies increase along the O, S, Se, and Te series both for the Zn and Cd compounds. In our theoretical results CdO nicely follows this general trend but the measured *d*-band energy, reported already 25 years ago,⁵⁶ grossly deviates from it. We do not think that these deviations originate from peculiarities related to the sixfold coordination in the rocksalt structure since we have obtained grossly improved band-structure results for the rocksalt compound NaCl, in general, as well by employing our pseudo-potentials.

All band structures shown in Figs. 8 and 9 have been calculated with our SIRC-PPs neglecting the relaxation shifts $\delta V_{\alpha}^{\Delta\text{SCF}}$ in the Zn 4s and Cd 5s pseudopotentials. These SIRC-PPs turn out to be most appropriate both on the basis of the general arguments given above and on the basis of the favorable results they yield in comparison with experiment. Comparing the SIRC-PP band structure of ZnO in the upper left panel of Fig. 8 with the respective SIC-PP band structure in the right panel of Fig. 4 we recognize that inclusion of electronic relaxation in V^{SIRC} further improves the *d*-band position and the gap energy but only has a marginal effect on the dispersions of the bands. We find the same conclusion to obtain for all other compounds studied. Significant changes in band dispersions relative to the standard pseudopotential LDA results are mainly brought about by δV^{SIC} . The additional $\delta V_{\alpha}^{\Delta\text{SCF}}$ corrections defining V^{SIRC} only give rise to small additional shifts of the band groups, changing their dispersions at most by 0.1 eV. In the lower left panel of Fig. 8, showing the band structure of *W* CdS, we have included the ARPES data of Stoffel⁵⁵ as well. Again we observe gratifying agreement between theory and experiment.

The different *W* band structures in Fig. 8 and the different ZB band structures in Fig. 9 show very similar topologies, respectively. The lower two panels of Fig. 8 allow for a direct identification of the changes induced by an exchange of the anions S and Se in the *W* Cd compounds. The same obtains for the upper two panels of Fig. 9 while the lower two panels of Fig. 9 exhibit the changes that occur when the cations Zn and Cd are exchanged in the tellurides. Comparing our band structures and the energy values in Table IV we observe that the gross features of the band structures of particular compounds are largely similar for the *W* and ZB modifications. The *d*-band energy positions and the widths of the anion-derived *p* valence bands are almost identical for both modifications. Only the gap energy for the *W* modifications turns out to be roughly 0.1 eV larger than that of the respective ZB modifications. The difference of some 0.1 eV results from all our calculations as well, in good agreement with experiment.

In view of the fact that the implementation of our pseudo-potentials V^{SIC} and V^{SIRC} does not increase the complexity of the respective LDA calculations in any way and, nevertheless, does yield much better results than standard pseudopotential LDA calculations, we consider the band structures

presented in this section as significant progress in electronic structure theory of II-VI compound semiconductors, indeed.

IV. EVALUATION OF THE TOTAL ENERGY

The description of structural parameters of solids within LDA employing standard pseudopotentials is usually in good agreement with experimental data. Therefore the question arises whether structural parameters like lattice constants and bulk moduli can equally well be described within LDA when our pseudopotentials are used. We first address the formal aspects of this question and then present related results.

A. Formalism for total-energy calculations

For the calculation of structural parameters we need the total energy of the system. It is a ground-state property on which electronic relaxation has no bearing. Thus in the context of total-energy calculations only self-interaction corrections need to be taken into account. In the framework of pseudopotential theory, the total energy is given within the full SIC-LDA approach²³ [cf. Eqs. (1) and (2) for SIC-LSD] as

$$E^{\text{SIC-LDA}}[n_v] = \sum_{\alpha}^{\text{occ}} \tilde{\varepsilon}_{\text{ps},\alpha}^{\text{SIC}} + \Delta E_1 + \Delta E_2, \quad (17)$$

with

$$\begin{aligned} \Delta E_1 = & -\frac{1}{2} \int V_{\text{Coul}}[n_v] n_v(\mathbf{r}) d^3 r + \int \varepsilon_{\text{xc}}^{\text{LDA}}[n_v] n_v(\mathbf{r}) d^3 r \\ & - \int V_{\text{xc}}^{\text{LDA}}[n_v] n_v(\mathbf{r}) d^3 r \end{aligned} \quad (18)$$

and

$$\begin{aligned} \Delta E_2 = & \sum_{\alpha}^{\text{occ}} \int \left\{ \frac{1}{2} V_{\text{Coul}}[n_{\alpha}] - \varepsilon_{\text{xc}}^{\text{LSD}}[n_{\alpha\uparrow,0}] + V_{\text{xc}}^{\text{LSD}}[n_{\alpha\uparrow,0}] \right\} \\ & \times n_{\alpha}(\mathbf{r}) d^3 r, \end{aligned} \quad (19)$$

where n_v and n_{α} are now the respective valence- and orbital-charge densities in the solid. Note that this SIC-LDA form of the total energy is not simply obtained by summing up the eigenvalues of Eq. (11) and correcting for double counting by ΔE_1 , as is usual in LDA. Within our approach we also have to incorporate the ΔE_2 term. This is the case, because we have approximated the full SIC contribution to the potential [cf. Eq. (4)], following from the linear variation of the full SIC-LDA total energy with respect to the one-particle orbitals, by $\delta \tilde{V}_{\alpha}^{\text{SIC}}$, i.e., by the nonlocal SIC contributions to our SIC-PPs. We can represent ΔE_2 by the following integral:

$$\Delta E_2 =: \sum_{\alpha}^{\text{occ}} \int \tilde{V}_{\alpha}[n_{\alpha}] n_{\alpha}(\mathbf{r}) d^3 r \quad (20)$$

involving the potential $\tilde{V}_{\alpha}[n_{\alpha}]$ whose definition becomes obvious from a direct comparison of Eqs. (19) and (20). From the solutions of Eq. (11) we can determine the valence-charge density n_v but we cannot resolve the orbital-charge densities n_{α} of the solid. In the same spirit as in Sec. II B we

use the *atomic* pseudocharge densities n_{α}^{at} instead of the orbital-charge densities n_{α} of the solid to evaluate the SIC contribution in ΔE_2 . This is consistent since the SIC contributions to the eigenvalues $\tilde{\varepsilon}_{\text{ps},\alpha}^{\text{SIC}}$ were evaluated the same way. We rewrite V_{α} as

$$\tilde{V}_{\alpha}[n_{\alpha}^{\text{at}}] =: V_{\alpha}[n_{\alpha}^{\text{at}}] + \frac{1}{r_{\text{loc}}} \quad (21)$$

and approximate V_{α} in complete analogy to Sec. II B 1 [cf. Eq. (10)] by the short-range potential

$$\begin{aligned} V_{\alpha}[n_{\alpha}^{\text{at}}] & \equiv \begin{cases} \frac{1}{2} V_{\text{Coul}}[n_{\alpha}^{\text{at}}] - \varepsilon_{\text{xc}}^{\text{LDA}}[n_{\alpha}^{\text{at}}] + V_{\text{xc}}^{\text{LDA}}[n_{\alpha}^{\text{at}}] - \frac{1}{r_{\text{loc}}}, & r \leq r_{\text{loc}} \\ 0, & r > r_{\text{loc}}. \end{cases} \end{aligned} \quad (22)$$

With $\tilde{\varepsilon}_{\text{ps},\alpha}^{\text{SIC}} = \varepsilon_{\text{ps},\alpha}^{\text{SIC}} - 2/r_{\text{loc}}$ according to Eq. (9) the appropriate total energy in our SIC-PP approach then reads

$$\begin{aligned} E^{\text{SIC-PP}}[n_v] = & \sum_{\alpha}^{\text{occ}} \varepsilon_{\text{ps},\alpha}^{\text{SIC}} - \frac{2N}{r_{\text{loc}}} - \frac{1}{2} \int V_{\text{Coul}}[n_v] n_v(\mathbf{r}) d^3 r \\ & + \int \varepsilon_{\text{xc}}^{\text{LDA}}[n_v] n_v(\mathbf{r}) d^3 r \\ & - \int V_{\text{xc}}^{\text{LDA}}[n_v] n_v(\mathbf{r}) d^3 r \\ & + \sum_{\alpha}^{\text{occ}} \int V_{\alpha}[n_{\alpha}^{\text{at}}] n_{\alpha}(\mathbf{r}) d^3 r + \frac{N}{r_{\text{loc}}}. \end{aligned} \quad (23)$$

Therefore in our approximate approach we do not need to evaluate the localized orbital-charge densities n_{α} as is necessary for a full SIC-LDA solid-state calculation of the total energy. The integrals involved in the calculation of ΔE_2 are solved for the solid by projecting the solid-state wave functions onto the localized atomic one-particle orbitals so that the respective term in Eq. (23) is approximated as

$$\begin{aligned} & \sum_{\alpha}^{\text{occ}} \int V_{\alpha}[n_{\alpha}^{\text{at}}] n_{\alpha}(\mathbf{r}) d^3 r \\ & \approx \sum_{n,\mathbf{k}} \left\langle \psi_{n,\mathbf{k}} \left| \sum_{\alpha} \frac{|\Phi_{\alpha}^{\text{ps}} V_{\alpha}\rangle \langle \Phi_{\alpha}^{\text{ps}} V_{\alpha}|}{\langle \Phi_{\alpha}^{\text{ps}} | V_{\alpha} | \Phi_{\alpha}^{\text{ps}} \rangle} \right| \psi_{n,\mathbf{k}} \right\rangle. \end{aligned} \quad (24)$$

This term can be calculated in a very efficient manner by representing the V_{α} as nonlocal, separable potentials (see the Appendix). The net constant $-N/r_{\text{loc}}$ occurring in Eq. (23) is a mere consequence of our choice of the reference energy for the eigenvalues $\varepsilon_{\text{ps},\alpha}^{\text{SIC}}$ in Eq. (9). It naturally enters and it improves the calculation of cohesive energies but it has no influence on the lattice constants or bulk moduli which follow from derivatives of the total energy. The total energy of the solid is then given by Eqs. (23) and (24) in general agreement with the respective SIC-LDA total energy of pseudoatoms. It is obtained from a self-consistent LDA calculation for the solid using our SIC-PPs which also provide the Bloch orbitals $\psi_{n,\mathbf{k}}$ for the calculation of ΔE_2 . For *pseudoatoms*, our respective results agree roughly within 0.1 eV with the

TABLE VI. Lattice constants a , c (in Å), and bulk moduli B (in Mbar) of W , RS, and ZB II-VI semiconductor compounds as calculated using standard pseudopotentials (PP) and our SIC pseudopotentials (SIC-PP) in comparison with experimental data from Ref. 48.

Table V		PP	SIC-PP	Expt.
ZnO ^W	a	3.23	3.29	3.25
	c	5.18	5.29	5.21
	B	1.60	1.59	1.43
ZnS ^W	a	3.71	3.83	3.82
	c	6.06	6.28	6.26
	B	1.02	0.83	0.76
ZnS ^{ZB}	a	5.25	5.42	5.41
	B	1.01	0.81	0.76
CdO ^{RS}	a	4.65	4.78	4.70
	B	1.72	1.52	
CdS ^W	a	4.03	4.15	4.13
	c	6.54	6.76	6.70
	B	0.87	0.74	0.61
CdS ^{ZB}	a	5.69	5.85	5.82
	B	0.87	0.70	
CdSe ^W	a	4.21	4.29	4.30
	c	6.86	7.02	7.01
	B	0.75	0.62	0.55
CdSe ^{ZB}	a	5.91	6.07	6.05
	B	0.79	0.66	
CdTe ^{ZB}	a	6.26	6.40	6.48
	B	0.79	0.52	

total energy resulting from full SIC-LDA calculations. Therefore the analogous approximation of the total SIC-LDA energy of the bulk system by Eqs. (23) and (24) is justified. Omitting the ΔE_2 term, on the contrary, leads to very inappropriate results both for pseudoatoms and for solids.

B. Results of total-energy calculations

We have applied the total-energy formalism described above to calculate lattice constants and bulk moduli for a set of W , RS, and ZB II-VI compounds. Of course, the usual ion-ion term is included in these calculations, as well. For comparison we have calculated the respective quantities also within the standard pseudopotential LDA approach. Our results are compared in Table VI with experimental data.⁴⁸ In general, we first note that the lattice constants resulting from our SIC-PP calculations are some 2% larger than those resulting from standard PP calculations. In particular, the lattice constants resulting with our SIC-PPs agree considerably better with experiment (except for ZnO and CdO) than the PP results. For most compounds considered they agree with experiment to within better than 1%. The increase of the lattice constants induced by SIC are related to the respective weakening of the p - d hybridization. An increased binding of the cationic semicore d states gives rise to a weakening of the chemical bond and a concomitant increase of the bond lengths and lattice constants. For the same reason the bulk moduli resulting with V_{ps}^{SIC} are smaller than those resulting with V_{ps}^{LDA} and agree considerably better with experiment

(except for ZnO, for which the improvement is only marginal). These general trends obtain likewise for both the ZB and W compounds. Similar effects on lattice constants and bulk moduli by inclusion of SIC have been observed previously for bulk Ce (Refs. 28 and 31) and bulk Ge (Ref. 34) as well.

V. SUMMARY AND OUTLOOK

We have reported the construction of SIC and SIRC pseudopotentials for II-VI compound semiconductors. The SIC-PPs, as compared to standard PPs, yield considerable improvements in the electronic structure of these compounds and they turn out to yield very reliable structural results for RS, ZB, and W II-VI compounds. While the SIC-PPs are most appropriate for the calculation of the ground-state energy of these solids they are not yet accurate enough to precisely describe semicore d -band positions and gap energies since they do not fully incorporate electronic relaxation. Electronic relaxation is then accounted for in our SIRC-PPs and they yield band-structure energies that are in gratifying agreement with experiment. Not only the d -band positions are satisfactorily described but also the gap energies in the more ionic compounds, for which our approximate approach is suited best, are in favorable agreement with the data. Small deviations remain only between calculated and measured d -band positions and gap energies for more covalent compounds, most noticeably for selenides and tellurides. For these our approximation to calculate the SIC contributions to the pseudopotentials by employing atomic orbital-charge densities instead of the solid-state orbital-charge densities becomes less appropriate. There are ways to further improve on this point and we are working on it.

The ideas and concepts developed in this paper are applicable, when appropriately generalized, to other classes of solids as well, as we plan to discuss in a future publication. Also for bulk NaCl, SiC, and GaAs we obtain considerable improvements in their electronic properties when calculated with our pseudopotentials. The improvements are most pronounced for the more ionic compounds NaCl and SiC and somewhat less impressive for GaAs. Even for Si or diamond improvements result within our current approach but they are relatively small as compared to those for the II-VI compounds, as was to be expected. Other very intriguing classes of solids that are most promising for an application of our SIC- and SIRC-PPs are transition metals and transition-metal oxides.

The key feature of our SIC- and SIRC-PP approach is the fact that it allows for straightforward *ab initio* LDA calculations of structural and electronic properties of semiconductors and insulators yielding results which agree very satisfactorily with the available experimental data. Nevertheless, they are not more involved than any ‘‘state of the art’’ LDA calculation for these solids.

ACKNOWLEDGMENT

We acknowledge financial support of this work by the Deutsche Forschungsgemeinschaft (Bonn, Germany) under Contract No. Po 215/9-1.

APPENDIX: SEPARABLE PSEUDOPOTENTIALS

In this appendix we briefly present the representation of the nonlocal pseudopotentials $V_{\text{ps},\alpha}^{\text{LDA}}$, $V_{\text{ps},\alpha}^{\text{SIC}}$, $V_{\text{ps},\alpha}^{\text{SIRC}}$, and V_α as separable pseudopotentials. Separable pseudopotentials, as suggested by Kleinman and Bylander,⁴⁴ are commonly used to reduce the computational load of an *ab initio* pseudopotential calculation. In order to obtain a specific nonlocal pseudopotential in separable form, each angular momentum (l) component is first separated into a local and a nonlocal (nl) part.

$$V_{\text{ps},l} = V_{\text{local}} + V_l^{\text{nl}}. \quad (\text{A1})$$

The choice of the local part is arbitrary. The separable Kleinman-Bylander form is given by

$$\begin{aligned} V_{\text{KB}}(r, r') &= V_{\text{local}}(r) \delta(r - r') \\ &+ \sum_l \sum_{m=-l}^l U_l(r) R_l(r) Y_{l,m}(\Theta, \varphi) Y_{l,m}^*(\Theta', \varphi') \\ &\times U_l(r') R_l^*(r'). \end{aligned} \quad (\text{A2})$$

The Y_{lm} are spherical harmonics and $R_l(r)$ are solutions of the radial Schrödinger equation

$$\left[-\frac{d^2}{dr^2} + \frac{l(l+1)}{r^2} + V_{\text{ps},l}(r) \right] r R_l(r) = E_l r R_l(r) \quad (\text{A3})$$

for a standard pseudopotential. The U_l are defined by

$$U_l(r) = \frac{V_{\text{ps},l}(r) - V_{\text{local}}(r)}{\left[\int R_l^*(r) [V_{\text{ps},l}(r) - V_{\text{local}}(r)] R_l(r) r^2 dr \right]^{1/2}}. \quad (\text{A4})$$

Our calculations are carried out employing Gaussian basis sets. The resulting potential matrix elements of the local part of (A2) are evaluated by transforming V_{local} into a Fourier representation. The remaining integrals involving two Gaussians and a plane wave are solved analytically. The matrix elements of the nonlocal potential are evaluated as described in the Appendix of Ref. 5.

In our standard LDA calculations we use for the anions the pseudopotentials from the tables of Gonze, Stumpf, and

Scheffler.⁴³ In these pseudopotentials the highest angular component is used as $V_{\text{local}}^{\text{LDA}}$. For the cations we use the pseudopotentials from the tables of Bachelet, Hamann, and Schlüter.⁴² In order to avoid ghost states and in order to create a very smooth local part of $V_{\text{KB}}^{\text{LDA}}$ we have chosen the $l=0$ components as $V_{\text{local}}^{\text{LDA}}$ for the cations. We obtain the radial wave function R_l^{LDA} from the solution of (A3) with $V_{\text{ps},l} = V_{\text{ps},l}^{\text{LDA}}$. Thus U_l^{LDA} is given by

$$\begin{aligned} U_l^{\text{LDA}}(r) &= \frac{V_{\text{ps},l}^{\text{LDA}}(r) - V_{\text{local}}^{\text{LDA}}(r)}{\left[\int R_l^{*\text{LDA}}(r) [V_{\text{ps},l}^{\text{LDA}}(r) - V_{\text{local}}^{\text{LDA}}(r)] R_l^{\text{LDA}}(r) r^2 dr \right]^{1/2}}. \end{aligned} \quad (\text{A5})$$

The SIC pseudopotential

$$V_{\text{ps},l}^{\text{SIC}} = V_{\text{ps},l}^{\text{LDA}} + \delta V_{\text{ps},l}^{\text{SIC}} \quad (\text{A6})$$

consists of the standard pseudopotential addressed above and the additional SIC contribution as detailed in Sec. II B 1. As local part of $V_{\text{KB}}^{\text{SIC}}$ we have chosen the local part of the standard pseudopotential $V_{\text{local}}^{\text{LDA}}$. We obtain the corresponding radial wave functions R_l^{SIC} from the solution of (A3) with $V_{\text{ps},l} = V_{\text{ps},l}^{\text{SIC}}$. Thus U_l^{SIC} is given in this case by

$$U_l^{\text{SIC}}(r) = \frac{V_{\text{ps},l}^{\text{SIC}}(r) - V_{\text{local}}^{\text{LDA}}(r)}{\left[\int R_l^{*\text{SIC}}(r) [V_{\text{ps},l}^{\text{SIC}}(r) - V_{\text{local}}^{\text{LDA}}(r)] R_l^{\text{SIC}}(r) r^2 dr \right]^{1/2}}. \quad (\text{A7})$$

The SIRC pseudopotentials including electronic relaxation (see Sec. II B 2) can be treated exactly the same way when $V_{\text{ps},\alpha}^{\text{SIC}}$ is replaced by $V_{\text{ps},\alpha}^{\text{SIRC}}$ and the wave functions R_l^{SIC} are replaced by R_l^{SIRC} .

The nonlocal terms in the potentials V_l , which are required to calculate the total energy of the bulk system using Eq. (24), are short ranged by construction. Thus in this case V_{local} is zero and the respective U_l is simply given by

$$U_l(r) = \frac{V_l(r)}{\left[\int R_l^{*\text{SIC}}(r) V_l(r) R_l^{\text{SIC}}(r) r^2 dr \right]^{1/2}}. \quad (\text{A8})$$

¹P. Hohenberg and W. Kohn, Phys. Rev. **136**, B864 (1964).

²W. Kohn and L. J. Sham, Phys. Rev. **140**, A1133 (1965).

³J. P. Perdew, R. G. Parr, M. Levy, and J. L. Balduz, Jr., Phys. Rev. Lett. **49**, 1691 (1982).

⁴M. Levy, J. P. Perdew, and V. Sahni, Phys. Rev. A **30**, 2745 (1984).

⁵P. Schröer, P. Krüger, and J. Pollmann, Phys. Rev. B **47**, 6971 (1993).

⁶P. Schröer, P. Krüger, and J. Pollmann, Phys. Rev. B **48**, 18 264 (1993).

⁷S. H. Wei and A. Zunger, Phys. Rev. B **37**, 8958 (1988).

⁸J. L. Martins, N. Troullier, and S. H. Wei, Phys. Rev. B **43**, 2213 (1991).

⁹Y. N. Xu and W. Y. Ching, Phys. Rev. B **48**, 4335 (1993), and see also the numerous references therein.

¹⁰Ch. Y. Yeh, S. H. Wei, and A. Zunger, Phys. Rev. B **50**, 2715 (1994).

¹¹M. Arai and T. Fujiwara, Phys. Rev. B **51**, 1477 (1995).

¹²S. B. Zhang, S. H. Wei, and A. Zunger, Phys. Rev. B **52**, 13 975 (1995).

¹³L. Ley, R. A. Pollak, F. R. McFelly, S. P. Kowalczyk, and D. Shirley, Phys. Rev. B **9**, 600 (1974).

¹⁴H. Lüth, G. W. Rubloff, and W. D. Grobman, Solid State Commun. **18**, 1427 (1976).

¹⁵W. Ranke, Solid State Commun. **19**, 685 (1976).

¹⁶G. Zwicker and K. Jacobi, Solid State Commun. **54**, 701 (1985).

¹⁷R. Weidmann, H. E. Gumlich, M. Kupsch, and H. U. Middelman, Phys. Rev. B **45**, 1172 (1992).

¹⁸M. S. Hybertsen and S. G. Louie, Phys. Rev. B **34**, 5390 (1986).

¹⁹M. Rohlfing, P. Krüger, and J. Pollmann, Phys. Rev. B **48**, 17 791 (1993); **52**, 1905 (1995).

- ²⁰O. Zakharov, A. Rubio, X. Blase, M. L. Cohen, and S. G. Louie, *Phys. Rev. B* **50**, 10 780 (1994).
- ²¹M. Rohlffing, P. Krüger, and J. Pollmann, *Phys. Rev. Lett.* **75**, 3489 (1995).
- ²²F. Aryasetiawan and O. Gunnarsson (unpublished).
- ²³J. P. Perdew and A. Zunger, *Phys. Rev. B* **23**, 5048 (1981).
- ²⁴L. Hedin and A. Johansson, *J. Phys. B* **2**, 1336 (1969).
- ²⁵J. A. Majewski and P. Vogl, *Phys. Rev. B* **46**, 12 219 (1992); **46**, 12 235 (1992).
- ²⁶A. Svane and O. Gunnarsson, *Phys. Rev. Lett.* **65**, 1148 (1990).
- ²⁷A. Svane, *Phys. Rev. Lett.* **68**, 1900 (1992).
- ²⁸A. Svane, *Phys. Rev. Lett.* **72**, 1248 (1994).
- ²⁹Z. Szotek and W. M. Temmermann, *Phys. Rev. B* **47**, 4029 (1993).
- ³⁰W. M. Temmermann and Z. Szotek, *Phys. Rev. B* **47**, 1184 (1993).
- ³¹Z. Szotek, W. M. Temmermann, and H. Winter, *Phys. Rev. Lett.* **72**, 1244 (1994).
- ³²D. Vogel, P. Krüger, and J. Pollmann, *Phys. Rev. B* **52**, R14 316 (1995).
- ³³A. Zunger, *Phys. Rev. B* **22**, 649 (1980).
- ³⁴M. M. Rieger and P. Vogl, *Phys. Rev. B* **52**, 16 567 (1995).
- ³⁵J. C. Slater, *The Self-consistent Field for Molecules and Solids* (McGraw-Hill, New York, 1974).
- ³⁶Throughout this paper we use the Rydberg energy as energy unit, if not stated otherwise.
- ³⁷J. G. Harrison, *J. Chem. Phys.* **78**, 4562 (1983).
- ³⁸M. R. Pederson and Chun L. Ling, *J. Chem. Phys.* **88**, 1807 (1989).
- ³⁹O. Gunnarsson and R. O. Jones, *Solid State Commun.* **37**, 249 (1981).
- ⁴⁰C. E. Moore, *Atomic Energy Levels*, Natl. Bur. Stand. (U.S.) Circ. No. 467 (U.S. GPO, Washington, DC, 1949), Vol. I; *ibid.* (U.S. GPO, Washington, DC, 1952), Vol. II; *ibid.* (U.S. GPO, Washington, DC, 1958), Vol. III.
- ⁴¹D. Vogel, Diploma thesis, Universität Münster, 1994 (unpublished).
- ⁴²G. B. Bachelet, D. R. Hamann, and M. Schlüter, *Phys. Rev. B* **26**, 4199 (1982).
- ⁴³X. Gonze, R. Stumpf, and M. Scheffler, *Phys. Rev. B* **44**, 8503 (1991).
- ⁴⁴L. Kleinman and D. M. Bylander, *Phys. Rev. Lett.* **48**, 1425 (1982).
- ⁴⁵J. Pollmann, P. Krüger, M. Rohlffing, M. Sabisch, and D. Vogel, in *Proceedings of the International Conference on the Formation of Semiconductor Interfaces (ISFSI-5)*, Princeton, New Jersey, edited by A. Kahn [*Appl. Surf. Sci.* **35**, 3170 (1996)].
- ⁴⁶D. M. Ceperley and B. J. Alder, *Phys. Rev. Lett.* **45**, 566 (1980).
- ⁴⁷D. J. Chadi and M. L. Cohen, *Phys. Rev. B* **8**, 5747 (1973).
- ⁴⁸*Semiconductors Physics of Group IV Elements and III-V Compounds*, edited by K. H. Hellwege and O. Madelung, Landolt-Börnstein, New Series, Group III, Vol. 17, Pt. a (Springer, Berlin, 1982); *Semiconductors. Intrinsic Properties of Group IV Elements and III-V-II-VI, and I-VII Compounds*, edited by K.-H. Hellwege and O. Madelung, Landolt-Börnstein, New Series, Group III, Vol. 22, Pt. a (Springer, Berlin, 1987).
- ⁴⁹The SIC pseudopotentials derived by Rieger and Vogl for Ge also give rise to \mathbf{k} -dependent band shifts (see Ref. 34).
- ⁵⁰U. Rossow, T. Werninghaus, D. R. T. Zahn, W. Richter, and K. Horn, *Thin Solid Films* **233**, 176 (1993).
- ⁵¹D. R. T. Zahn, G. Kudlek, U. Rossow, A. Hoffmann, I. Broser, and W. Richter, *Adv. Mater. Opt. Electron.* **3**, 11 (1994).
- ⁵²K. O. Magnusson and S. A. Flodström, *Phys. Rev. B* **38**, 1285 (1988).
- ⁵³K. O. Magnusson (private communication).
- ⁵⁴Of course, one could easily arrive at gap energies and d -band positions for the selenides and tellurides as well that practically agree with experiment by respective *ad hoc* choices of the $\Delta\tilde{V}_\alpha^{\text{ASCF}}$ contributions to the $4p$ and $5p$ pseudopotentials of Se and Te, respectively. Doing so would be very sensible from a practical point of view and should turn out to be useful, e.g., in the context of actual calculations of particular bulk defect or surface and interface properties. But it would mean leaving our well-defined theoretical framework and introducing the relaxation-induced shift of the anion p states to a certain extent as an empirical parameter in the SIRC-PPs. In this work we refrain from such an empirical procedure.
- ⁵⁵N. G. Stoffel, *Phys. Rev. B* **28**, 3306 (1983).
- ⁵⁶C. J. Vesely and D. W. Langer, *Phys. Rev. B* **4**, 541 (1971).